METEOR-Berichte

AMOC Components at 47°N

Cruise No. M164 (GPF-19-1-105)

June 23 – July 31, 2020
Emden (Germany) – Emden (Germany)

D. Kieke, K. Bulsiewicz, C. Gapp, Y. Hinse O. Huhn, B. Holanda, A. Hunkemöller, S. Kinne, M. Köllner, L. Krisztian, O. Krüger, I. Leimann, M. Pöhlker, A. Schneehorst, A. Smirnov, R. Steinfeldt, M. Stelzner, J. Stiehler, T. Svensson, S. Wett, K. N. Wiegand

Chief Scientist: Dr. Dagmar Kieke

University of Bremen

2021

Table of Contents

1 Summary

Cruise *M164 (GPF-19-1-105)* with *R/V METEOR*, in the following abbreviated as *M164*, focused on investigating the strength and the variability of the oceanic current field in the southern and central subpolar gyre of the North Atlantic. Emphasis was put on studying the intra- to interannual variability of the oceanic circulation system and subtropical or subpolar water masses imported and exported across the latitude of about 47°N. The overall aim of the cruise was to gain suitable physical oceanographic data from ship-based observations and moored sensors that serve to further extend in time already existing time series of current system volume transports and water mass properties. These are needed to infer an estimate of the overall strength of the Atlantic Meridional Overturning Circulation (AMOC) at 47°N.

One focus of the cruise was on recovering the instrumental components of the long-term observational array NOAC ("North Atlantic Changes"). NOAC consisted of deep-sea moorings that were located in the western and eastern boundary current regions of the North Atlantic, as well as inverted echo-sounders equipped with pressure sensors (PIES) that were installed in the deep basins along 47°/48°N. As NOAC was to be decommissioned in 2020, the western deep-sea mooring and eight PIES were recovered without replacement. Two deep-sea moorings located at the eastern boundary of the North Atlantic were recovered and subsequently redeployed.

A second focus dealt with basin-wide hydrographic observations along two sections, with one spanning the deep North Atlantic along 47°/48°N and a second one located on the western flank of the Mid-Atlantic Ridge (MAR). These sections form important gateways as they cross major pathways associated with the north- and eastbound North Atlantic Current (NAC) and its recirculation branches. Furthermore, they cover the export routes of North Atlantic Deep Water (NADW) as it spreads towards the subtropics or crosses the MAR. Work at these stations included conductivity-temperature-depth-oxygen (CTDO) profiling and analysis of water samples to calibrate the corresponding conductivity and oxygen sensors. Furthermore, water samples were taken at most stations and measured on board with respect to analysing the oceanic content of anthropogenic tracers such as sulphur hexafluoride (SF_6) and chlorofluorocarbons (CFC) throughout the water column. Lowered and vessel-mounted Acoustic Doppler Current Profiler devices (LADCP and VMADCP) delivered station-based and continuously measured data of the oceanic velocity field.

In total, 126 CTDO and LADCP stations were carried out during cruise *M164*. Seven Argo floats of type *NKE Arvor I* and eight floats of type *NKE Deep Arvor* were deployed along 47°/48°N as part of the international Argo programme. Eight PIES and three deep-sea moorings were recovered, two moorings were redeployed again at the eastern margin.

Zusammenfassung

Die Fahrt *M164 (GPF-19-1-105)* mit *FS METEOR*, im Folgenden abgekürzt als *M164*, diente der Untersuchung der Stärke und der Variabilität des ozeanischen Strömungsfeldes im südlichen und zentralen subpolaren Wirbel des Nordatlantiks. Der Schwerpunkt lag auf der Untersuchung der intra- bis interannualen Variabilität des ozeanischen Zirkulationssystems und der subtropischen bzw. subpolaren Wassermassen, die über den 47°N-Breitengrad importiert und exportiert werden. Das übergeordnete Ziel der Fahrt war die Gewinnung geeigneter physikalisch-ozeanographischer Daten aus schiffsgestützten Beobachtungen und verankerten Sensoren, die dazu dienen, die bereits vorhandenen Zeitreihen der Volumentransporte des Strömungssystems und der Wassermasseneigenschaften zeitlich zu verlängern. Diese werden benötigt, um die Gesamtstärke der Atlantischen Meridionalen Umwälzzirkulation (AMOC) bei 47°N abzuleiten.

Ein Schwerpunkt der Reise lag auf der Bergung der instrumentellen Komponenten des Langzeitbeobachtungsarrays NOAC ("North Atlantic Changes"). NOAC bestand aus Tiefsee-Verankerungen, die sich in den westlichen und östlichen Randstromgebieten des Nordatlantiks befanden, sowie aus mit Drucksensoren ausgestatteten invertierten Boden-Echoloten (PIES), die in den tiefen Becken entlang 47°/48°N installiert waren. Da das NOAC-Observatorium im Jahr 2020 außer Betrieb genommen werden sollte, wurden die westliche Tiefseeverankerung und acht PIES ersatzlos geborgen. Zwei Tiefseeverankerungen an der östlichen Grenze des Nordatlantiks wurden geborgen und anschließend wieder ausgelegt.

Ein zweiter Schwerpunkt waren beckenweite hydrographische Beobachtungen entlang zweier Schnitte, wobei einer den tiefen Nordatlantik entlang 47°/48°N überspannt und ein zweiter an der Westflanke des Mittelatlantischen Rückens (MAR) verläuft. Diese Schnitte bilden wichtige Schlüsselstellen, da sie die Pfade kreuzen, die mit dem nord- und ostwärts gerichteten Nordatlantikstrom (NAC) und seinen Rezirkulationszweigen verbunden sind. Außerdem decken sie die Exportrouten des Nordatlantischen Tiefenwassers (NADW) ab, wenn es sich in Richtung Subtropen ausbreitet oder den MAR überquert. Die Arbeiten an diesen Stationen umfassten die Erhebung von Leitfähigkeits-Temperatur-Tiefen-Sauerstoff-Profilen (CTDO) und die Analyse von Wasserproben zur Kalibrierung der entsprechenden Leitfähigkeits- und Sauerstoffsensoren. Außerdem wurden an den meisten Stationen Wasserproben entnommen und an Bord gemessen, um den ozeanischen Gehalt an anthropogenen Tracern wie Schwefelhexafluorid (SF_6) und Fluorchlorkohlenwasserstoffen (FCKW) in der gesamten Wassersäule zu analysieren. Gefierte und schiffsgebundene Doppler-Strömungsprofil-Messgeräte (LADCP und VMADCP) lieferten stationsbasierte und kontinuierlich gemessene Daten des ozeanischen Geschwindigkeitsfeldes.

Insgesamt wurden während der Fahrt *M164* 126 CTDO- und LADCP-Stationen durchgeführt. Sieben Tiefendrifter vom Typ *NKE Arvor I* und acht Tiefendrifter vom Typ *NKE Deep Arvor* wurden im Rahmen des internationalen Argo-Programms entlang von 47°/48°N ausgebracht. Acht PIES- und drei Tiefsee-Verankerungen wurden geborgen, zwei Verankerungen wurden am östlichen Rand wieder ausgebracht.

2 Participants

Name	Discipline	Institution
Kieke, Dagmar, Dr.	chief scientist	IUPHB/MARUM
Bulsiewicz, Klaus	tracer sampling and analysis	IUPHB
Gapp, Cyril	CTDO/LADCP	IUPHB/MARUM
Hinse, Yannik	tracer sampling and analysis	IUPHB/MARUM
Huhn, Oliver, Dr.	tracer sampling and analysis	IUPHB
Hunkemöller, Annette	CTDO/LADCP	IUPHB/MARUM
Köllner, Manuela	mooring preparation and analysis	BSH
Krisztian, Lina	CTDO/LADCP	IUPHB/MARUM
Leimann, Ilmar	CTDO/LADCP, vmADCP data processing, mooring assistance	IUPHB/MARUM
Schneehorst, Anja	mooring preparation, technics, float deployments	BSH
Steinfeldt, Reiner, Dr.	CTDO data processing, calibration and data analysis, salinometry, oxygen titration	IUPHB
Stelzner, Martin	meteorology	DWD
Stiehler, Jan Eric	CTDO/LADCP, vmADCP data processing	IUPHB/MARUM
Svensson, Tobias	mooring preparation, technics, float deployments	BSH
Wett, Simon	PIES processing, oxygen titration	IUPHB/MARUM
Wiegand, Kevin Niklas	LADCP data processing, data evaluation	IUPHB/MARUM

BSH	Federal Maritime and Hydrographic Agency, Hamburg, Germany
DWD	German Weather Service, Hamburg, Germany
IUPHB	University of Bremen, Institute of Environmental Physics, Bremen, Germany
MARUM	University of Bremen, Centre for Marine Environmental Sciences, Bremen, Germany

As part of the of the obligatory safety measures in connection with the global COVID19 pandemic prevailing in 2020, the scientific team during cruise *M164* had to be smaller than usual. Consequently, the team size had to be reduced to sixteen scientific participants.

3 Research Program

As during previous cruises, scientific work during cruise *M164* focused on collecting physical-oceanographic data along the geographic latitude of ~47°/48°N as well as along the western flank of the Mid-Atlantic Ridge.

Activities during the cruise dealt with mostly recovering and partly redeploying the moored core components of the long-term transport array NOAC. Data (station-based and underway data) were acquired in order

- to observe and determine the strength of the deep water export across 47°/48°N in 2019 to 2020;
- to measure and quantify the respective strength regarding northward import of warm and saline water with the North Atlantic Current (NAC) into the subpolar gyre in this period;
- to determine the portion of the NAC that crosses the Mid-Atlantic Ridge into the eastern basin in 2020, and to what degree is it linked to the location and variation of the Subpolar Front;
- to quantify how much Labrador Sea Water (LSW) leaves the subpolar North Atlantic across 47°N and propagates into the eastern basin, and what are its present water mass characteristics;
- to refurbish and/or recover the moored components of the long-term observational observatory NOAC (North Atlantic Changes) deployed along ~47°/48°N.

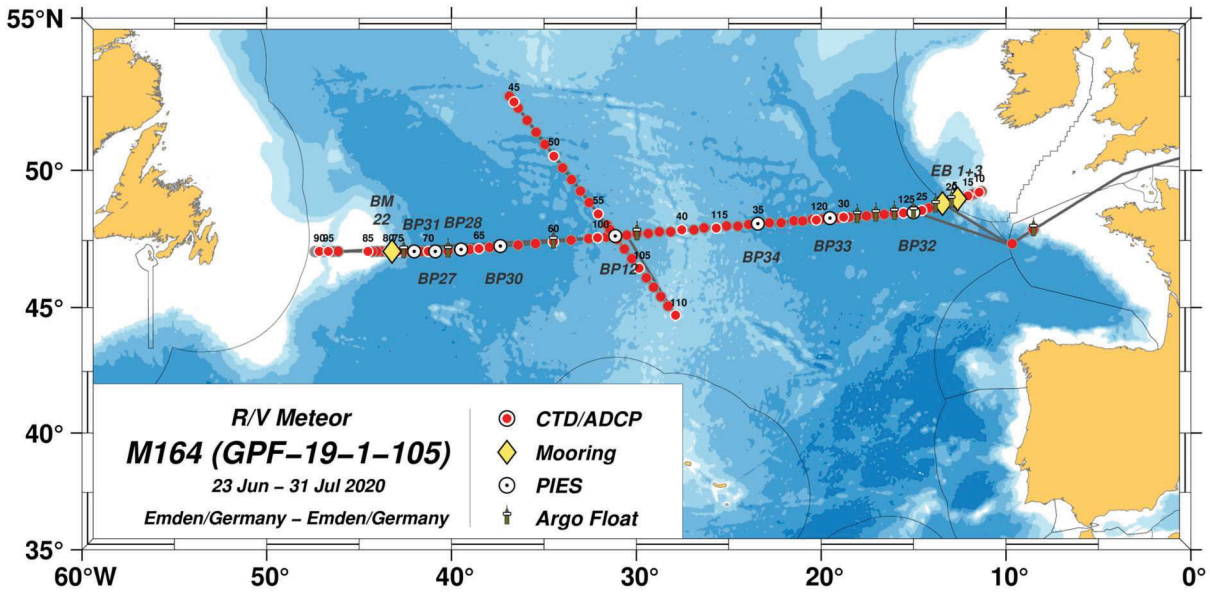

Fig. 3.1 Track chart of *R/V METEOR* cruise *M164 (GPF-19-1-105)*. Numbers indicate hydrographic profiles, alpha-numeric labels refer to mooring and PIES identifiers.

4 Narrative of the Cruise

Due to the global COVID19 pandemic prevailing in 2020, the original port calls in Brest, France, and St. John's, Canada, were canceled. Instead, the entire German scientific fleet was

supposed to sail from and to German ports only for the time being. After having passed a quarantine phase and having been tested negatively for the Corona virus, all cruise participants were allowed to enter the vessel and started setting up laboratories and installing the necessary scientific equipment. *R/V METEOR* left its berth in Emden, Germany, on June 23, 2020, at 07:12 UTC. The scientific mission of cruise *M164* started on June 25 at 07:30 UTC, when continuous logging of underway data was switched on. Course was set towards the western edge of the French EEZ. There, a number of test stations were carried out in deep water during June 25 and 26, and a first profiling Argo float was deployed. These test stations served to check the performance of the conductivity-temperature-depth-oxygen (CTDO) unit and the two Lowered Acoustic Doppler Current Profilers (LADCP) attached to the carousel water sampler. Furthermore, the functioning of acoustic releases at depth was verified as well as first calibration casts for moored sensors were carried out. Between June 27 and July 1, we conducted a high-resolution CTDO/LADCP section along the crest of the topographic obstacle named Goban Spur and started tracer sampling and data analysis. We also recovered and subsequently redeployed the two deep-sea moorings *EB-1* and *EB-3* and performed acoustic telemetry on the bottom-mounted pressure-sensor-equipped inverted echo-sounder (PIES) *BP-32*. This device was subsequently recovered without replacement. In the following, we headed across the West European Basin along 47°/48°N and continued the hydrographic sampling program as well as work on two additional PIES, *BP-33* and *BP-34*, with the first one to be recovered as well. Acoustic telemetry did not work regarding the latter. Due to worsening weather conditions, we postponed the recovery of the device to the end of the cruise.

Having arrived at PIES-station *BP-12* on July 6 2020, we changed to a northwestern course and headed north along the western flank of the Mid-Atlantic Ridge (MAR). On July 8, we resumed hydrographic measurements at the northern end of this line and, while doing station work, headed back along the same line towards the 47°/48°N section.

Between July 12 and July 17, we followed a westward course towards Flemish Cap, while performing hydrographic stations, acoustic work on the PIES *BP-27*, *BP-28*, *BP-30*, and *BP-31* including the recovery of all devices, and recovery of the mooring *BM-22*. After transiting across Flemish Cap, fieldwork continued in the Flemish Pass on July 18 and 19. There, we carried out a hydrographic section across the width of the passage and started to transit towards the eastern basin of the Atlantic Ocean.

On July 20, we reached the vicinity of the MAR again and continued the previously made section along the western flank of the ridge in southeastern direction. On July 22, we were back on the 47°/48°N section and continued hydrographic station work towards the eastern end of the section. The last remaining PIES, *BP-34,* located in the West European Basin, was recovered on July 25. Hydrographic station works finally ended on July 27, 2020. After all fieldwork was finished, we headed east towards Emden, Germany.

Continuous logging of underway data was stopped on July 29, 02:45 UTC, which marked the end of the scientific mission of cruise *M164* aboard *R/V METEOR*. On July 31, the vessel arrived at the pilot station of Emden, Germany, and was finally towed at the pier in Emden port the same day.

In total, 126 hydrographic profiles were carried out during cruise *M164*. Eight PIES and three deep-sea moorings were recovered, and two moorings were subsequently reinstalled again. Seven Argo floats of type *NKE Arvor I* and eight floats of type *NKE Deep Arvor* were deployed along 47°/48°N. While the first group was programmed to drift at a parking depth of 1000 dbar and to cycle between 2000 dbar and the sea surface every ten days, the second group of floats was programmed to drift at a parking depth of 2750 dbar and to cycle between 4000 dbar and the sea surface.

5 Preliminary Results

5.1 CTDO Measurements and Sensor Calibration

(R. Steinfeldt, S. Wett, C. Gapp, A. Hunkemöller, M. Köllner, L. Krisztian, I. Leimann, A. Schneehorst, J. Stiehler)

5.1.1 CTDO System and Performance

Conductivity, temperature, depth (pressure), and oxygen (CTDO) were measured at all stations with a profiling device of type *Seabird Electronics (SBE) 9/11 plus* and an *SBE-43* dissolved oxygen sensor. All devices in use are listed in Table 5.1. The CTD was mounted to a water sampler frame with 22 Niskin bottles of 10 l volume and two lowered Acoustic Doppler Current Profilers (LADCP). Water from the Niskin bottles was analysed with respect to the anthropogenic tracers CFC-12 and SF_6. In addition, oxygen and salinity samples were collected, mainly to calibrate the conductivity and oxygen sensors. Depending on the water depth, 2-4 salinity and 2-7 oxygen samples (including one double sample) were taken at each station. The CTD system worked properly throughout the whole cruise. Only at station/profile #017/019, the downcast was terminated precociously due to a failure of the ship's outrigger that was used to deploy and recover the CTDO/water sampler system.

Tab. 5.1 Overview on CTDO devices and sensors used during cruise *M164*.

Device	Serial Number
SBE 09plus	09p26816-0657
SBE 11plus, deck unit	11p26816-0598
"Digiquartz" pressure sensor	86532
SBE 03plus, temperature sensor	03P-4145 & 03P-4156
SBE 04C, conductivity sensor	04-2646
SBE 05T, submersible pump	05-3138
SBE 43, dissolved oxygen sensor	43-0267
Altimeter, *Benthos* PSA-916, 200 kHz	75743
Mechanical bottom alert	-

All derived salinities refer to the Practical Salinity Scale *PSS-78*, all respective densities have been inferred from the *EOS-80* equation. A pressure offset of the CTD sensor of 0.4 dbar was

determined from the recorded pressure data at the beginning of the CTD casts, and the CTD pressure was corrected accordingly. The (preliminary) calibrated CTD data of the upper 4000 m in a resolution of 5 dbar were sent during the cruise in near-real-time to the *Coriolis* data centre at *Ifremer*, Brest, France.

5.1.2 CTDO Sensor Calibration

Conductivity/Salinity

The salinity samples from the Niskin bottles were measured by means of a salinometer, type *Guildline Autosal 8400A* (s/n 59.083). At the beginning of each measurement session, the salinometer was standardized with a IAPSO seawater, batch P162. This procedure only led to minor adjustments of the standardization potentiometer. During the sessions, repeated measurements of substandard (water collected from Niskin bottles closed at the same location) did not show a drift of the salinometer. The accuracy based on the repeated measurements of substandard was about 0.0007.

The calibration of the conductivity sensor resulted in a small correction of the order of $3 \cdot 10^{-3}$ mS/cm. In addition, the deviation of the CTD towards the measured salinity samples increased over the duration of the cruise by about $2 \cdot 10^{-3}$ mS/cm. The full calibration string is given in Tab. 5.2 and encompasses a constant offset and terms proportional to time and conductivity. The rms error of the calibrated CTD and the bottle salinity is about 0.0019 (0.0017 for samples below 1000 dbar), see Figs. 5.1 and 5.2. Considering the uncertainty of the salinometer and the standard seawater batch (~0.001), the precision of the CTD salinity data from this cruise is about 0.0025.

Fig. 5.3 shows the T/S diagram (deepest part of the profiles only) for profiles located between 16°W and 14°30'W along the 47°N/48°N section taken from cruises conducted between 2016 to 2020. During the cruise *M164*, CTD casts have been performed at the beginning of the cruise along the eastern part, when heading westward, and towards the end, when heading eastward, with a time difference of more than 3 weeks. The T/S diagram (Fig. 5.3) does not show any difference in the bottom layer between the calibrated CTD data of these two periods. Also, the difference towards the previous cruises is smaller than the uncertainty of the CTD salinity.

Tab. 5.2 Calibration string applied to conductivity data recorded during cruise *M164*. "C" refers to conductivity, sensor #04-2646.

M164 CTD-Station/Profile	Conductivity Calibration String
#001/001 - #128/126	C_{corr} = C - 1.117705898415312e-02 + 9.536887971385429e-05*time - 1.145341155605751e-04*C

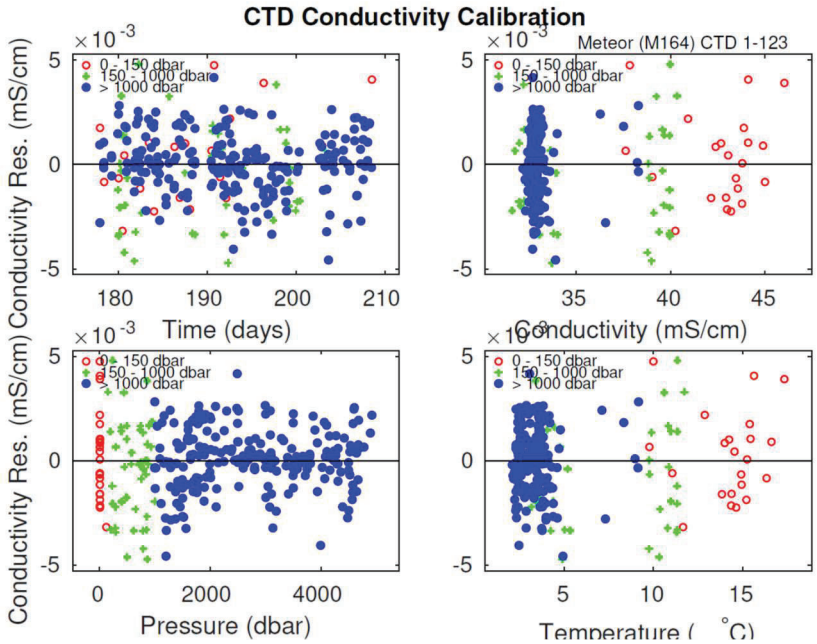

Fig. 5.1 Conductivity residuals between calibrated CTD conductivity and conductivity from measured salinity samples for stations/profiles #001/001 - #125/123 (conductivity sensor #04-2646), cruise *M164*.

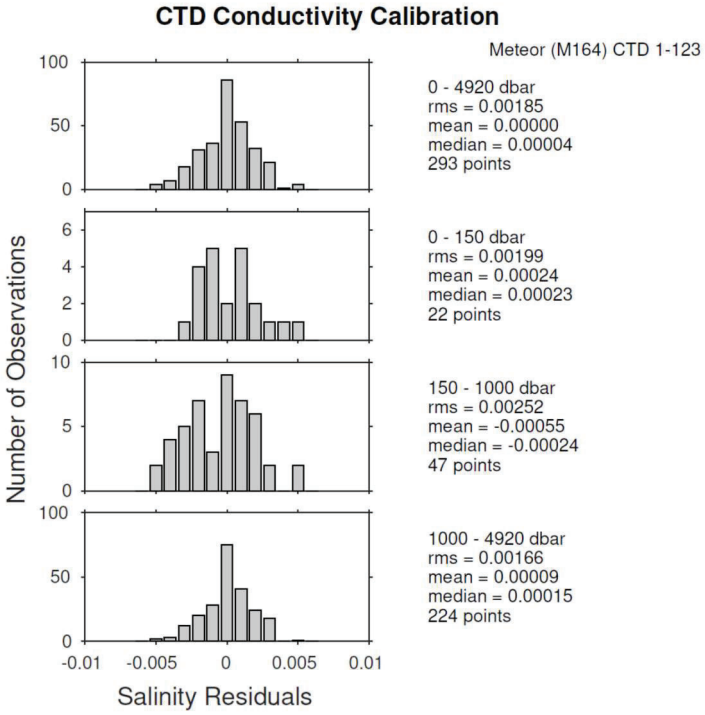

Fig. 5.2 Histogram of salinity residuals for CTD stations/profiles #001/001 - #125/123 (conductivity sensor #04-2646).

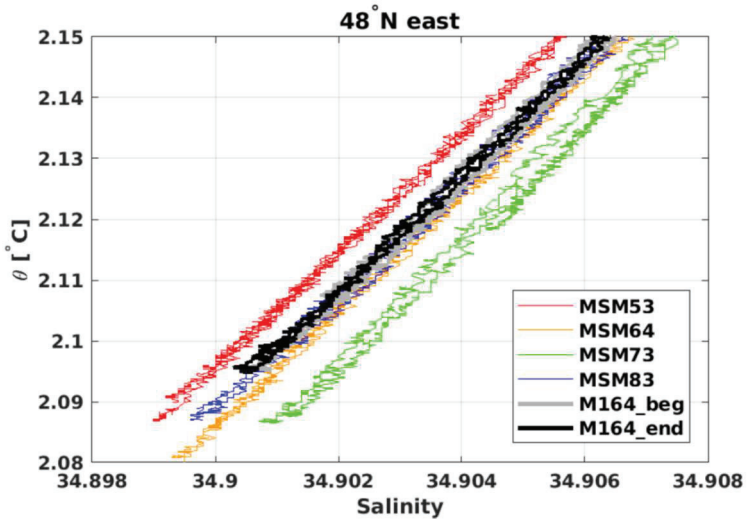

Fig. 5.3 T-S-diagram for the bottom water of the eastern part of the 47°/48°N section for cruises from 2016 (*MSM53*), 2017 (*MSM64*), 2018 (*MSM73*), 2019 (*MSM83*), and the beginning and end of cruise *M164* (2020).

Oxygen

The *SBE-43* dissolved oxygen sensor was calibrated by using the data from the bottle oxygen measured by Winkler titration. During the first period of the cruise, when heading westward, the oxygen sensor showed a temporal drift. When the CTD casts started again near the Mid-Atlantic Ridge after two days of transit, this temporal trend was no longer visible. Thus, the calibration of the sensor was done separately for the station/profiles #001/001 - #101/099 and #102/100 - #128/126. Figures 5.4 and 5.5 show the results of the calibration for the first period, which includes more bottle oxygen data. The calibration strings for both periods are given in Table 5.3.

The rms error between the calibrated CTD oxygen and the bottle data from Winkler titration was about 0.45 ml/l (~0.75%) for all samples and decreased to 0.38 ml/l (~0.6%) if only samples below 1000 dbar were considered. This result holds for both calibration periods. Together with the uncertainty of the bottle oxygen of ~0.5%, the total error of the CTD oxygen is below 1.%.

Tab. 5.3 Calibration string applied to oxygen data recorded by the CTD oxygen sensor during cruise *M164*. "O" refers to dissolved oxygen (sensor #43-0267), "P" to pressure.

M164 CTD-Stations/Profiles	Oxygen Calibration String
#001/001-#101/099:	O_{corr} = O - 3.990496941700103e-01 + 3.783929089191199e-03*time + 2.281411845294646e-05*P
#102/100-#128/126:	O_{corr} = O + 2.885714930937223e-01 + 2.502984731906863e-02*O + 1.773861475719939e-06*P

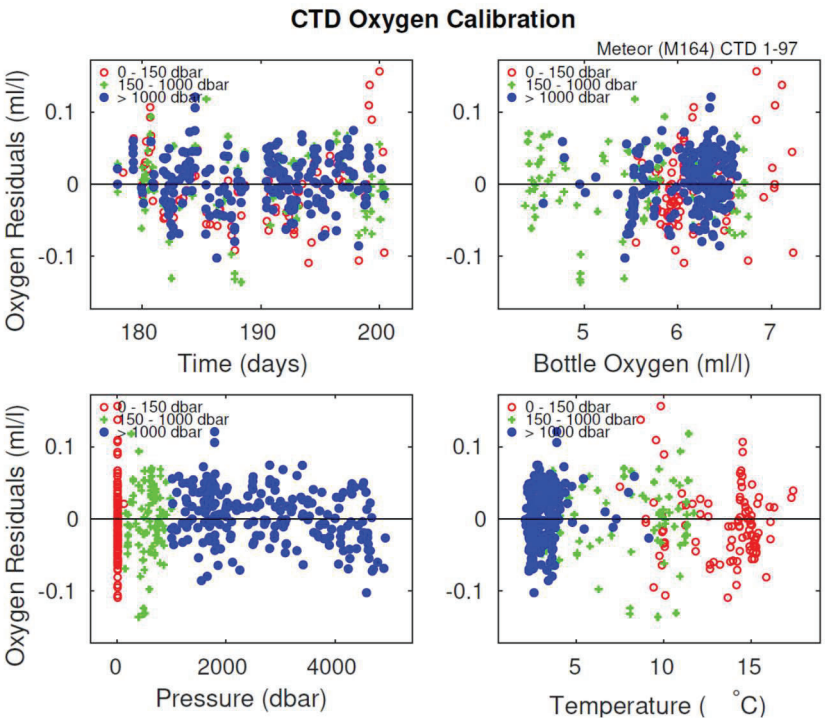

Fig. 5.4 Oxygen residuals between calibrated CTD-derived oxygen and oxygen from measured water samples for stations #001/001 - #099/097 (oxygen sensor #43-0267), cruise *M164*.

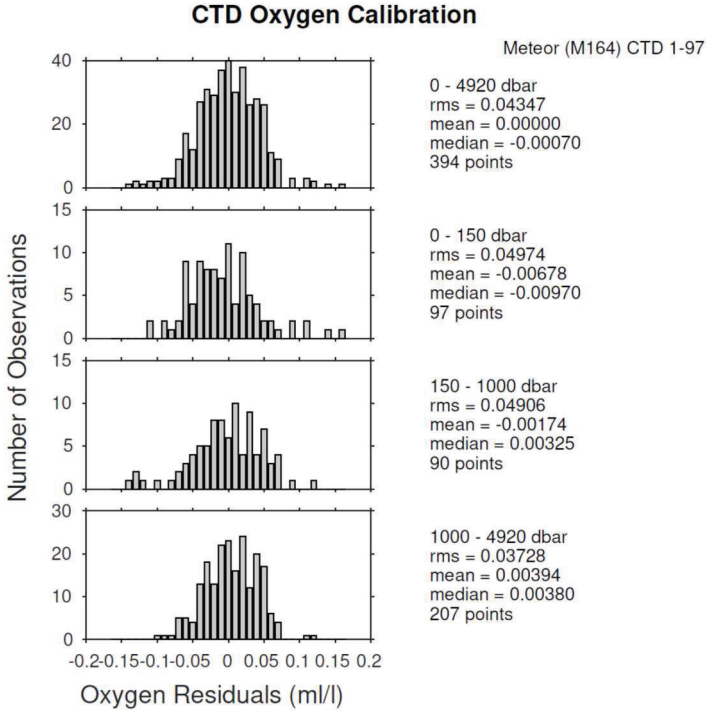

Fig. 5.5 Histogram of residuals between calibrated CTD oxygen and bottle data analyzed by Winkler titration, stations #001/001 - #099/097, oxygen sensor #43-0267, cruise *M164*.

Fig. 5.6 shows the comparison of the oxygen profiles from the eastern part of the 47/48°N section between 16°W and 14°30'W. As mentioned above, CTD casts in this region were performed at the beginning and end of this cruise. Towards the bottom, no significant difference can be seen. A detailed analysis reveals differences of 0.02 ml/l for the oxygen from the two periods of this cruise, which is smaller than the uncertainty of 1%. The same holds for the comparison with the cruises from the previous years, starting with *MSM53* in 2016. In the density range of the Labrador Sea Water (LSW), around σ_θ =27.75 kg/m³, the profiles from this cruise show some extreme features. At the beginning of the cruise, one profile indicated the intrusion of Mediterranean Outflow Water with high salinity and low oxygen. The admixture of this water also led to instabilities in the potential density referenced to the surface. During the end of the cruise, one profile was strongly influenced by the eastward penetration of oxygen-rich LSW.

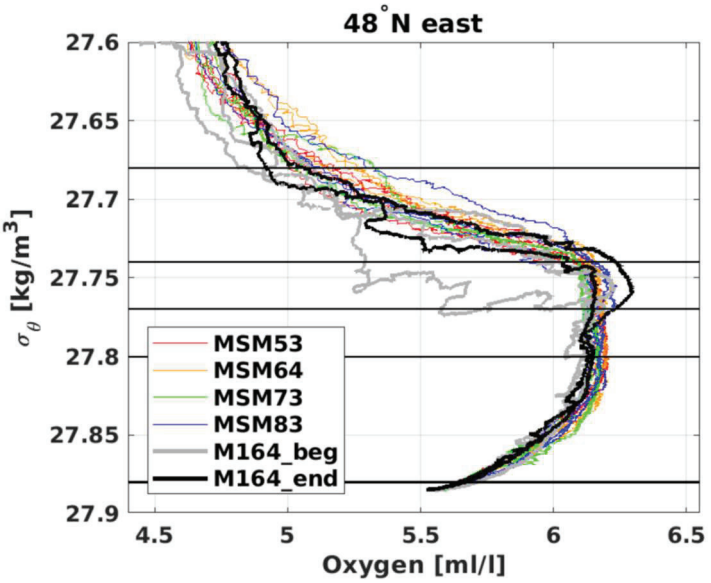

Fig. 5.6 Oxygen profiles from the eastern part of the 47°/48°N section for cruises from 2016 (*MSM53*), 2017 (*MSM64*), 2018 (*MSM73*), 2019 (*MSM83*) and the beginning and end of cruise *M164* (2020) plotted vs. potential density σ_Θ.

5.1.3 Analysis of Bottle Oxygen

(R. Steinfeldt, S. Wett)

In order to calibrate the oxygen sensor of the CTDO unit, oxygen samples taken from the Niskin bottles were analyzed. Depending on the depth of the CTD stations, 2-7 samples per station were taken. In case of very dense station spacing, every second station was skipped. In total, 591 samples were analyzed, including 64 double samples.

The method used for the analysis of oxygen dissolved in seawater is based on the Winkler procedure for the determination of dissolved oxygen in sea water. After drawing the sample, the oxygen was fixated by adding 1 ml manganese(II)-chloride ($MnCl_2$) with the concentration of 200 g in 500 ml of pure water and 1 ml of alkaline solution (NaOH-KI) with a concentration of

180 g of sodium hydroxide (NaOH) and 75 g of potassium iodide (KI) in 500 ml of distilled water. Before measuring, 1 ml of 50% sulfuric acid (H_2SO_4) needed to be added. The titration itself was performed by a *Schott TitroLine alpha* titration system, where the endpoint of the titration was determined by measuring the voltage at the instrument's electrode. As titer solution, sodium thiosulfate ($Na_2S_2O_3$) with a normality of 0.02 N was used. This solution was made from a mother solution of 0.1 N $Na_2S_2O_3$, which was diluted by 1:5. The 0.1 N $Na_2S_2O_3$ mother solution was renewed 3 times during the cruise, the 0.02 N $Na_2S_2O_3$ titer every few days.

The standardization of the sodium thiosulfate was performed by a 0.1 N KIO_3 solution. This standard was titrated every day before and after the measurements of the oxygen samples. After diluting 1 ml of the potassium iodate standard in pure water, 1 ml of sulfuric acid and 5 ml of a 10% KI solution were added, and then a normal titration was performed. Theoretically, for 1 ml of KIO_3 5 ml of $Na_2S_2O_3$ are needed. With the S*chott TitroLine* device used on this cruise, the amount of $Na_2S_2O_3$ was about 4% higher. About 4 standard determinations were performed per measurement session with a mean standard deviation of 0.017 ml $Na_2S_2O_3$ or about 0.3%. From day to day, the standard measurements showed a variability in the order of < 1%. When renewing the 0.02 N $Na_2S_2O_3$ titer, no significant change of the standard measurements could be detected. The rms error of the double samples (0.2%) combined with the uncertainty of the standard determination results in a precision of the bottle oxygen values of about 0.5 %.

In the surface layer, oxygen was oversaturated over the whole cruise (Fig. 5.7), probably due to primary production and surface warming. Between profiles #072/070 and #101/099, i.e. along the western part of the 47°/48°N section, the bottle oxygen in the surface layer often showed a higher oversaturation compared to the CTD oxygen (Fig. 5.7). This can be explained by the shallowing of the mixed layer due to weak winds and seasonal warming. The uppermost Niskin bottles were closed at around 14 m during a short stop during the upcast. The lower mixed layer boundary was often located directly below that depth. In these cases, the CTD measured the higher temperatures and lower oxygen of the mixed layer. The Niskin bottles, however, still contained remnants of cold, oxygen rich water from below the mixed layer, as the short stopping time is not sufficient for a complete exchange of the water within the bottles. This leads to the 'apparent' high oversaturation of the bottle oxygen.

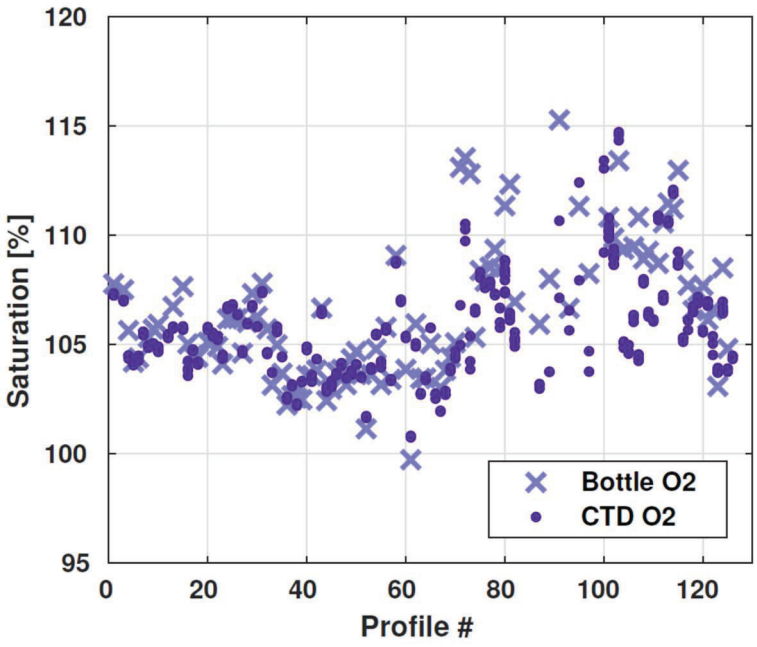

Fig. 5.7 Saturation [%] of bottle oxygen samples and CTDO-derived oxygen in the surface layer (< 25 m).

5.2 Sampling and Analysis of Transient Tracers

(K. Bulsiewicz, O. Huhn, Y. Hinse)

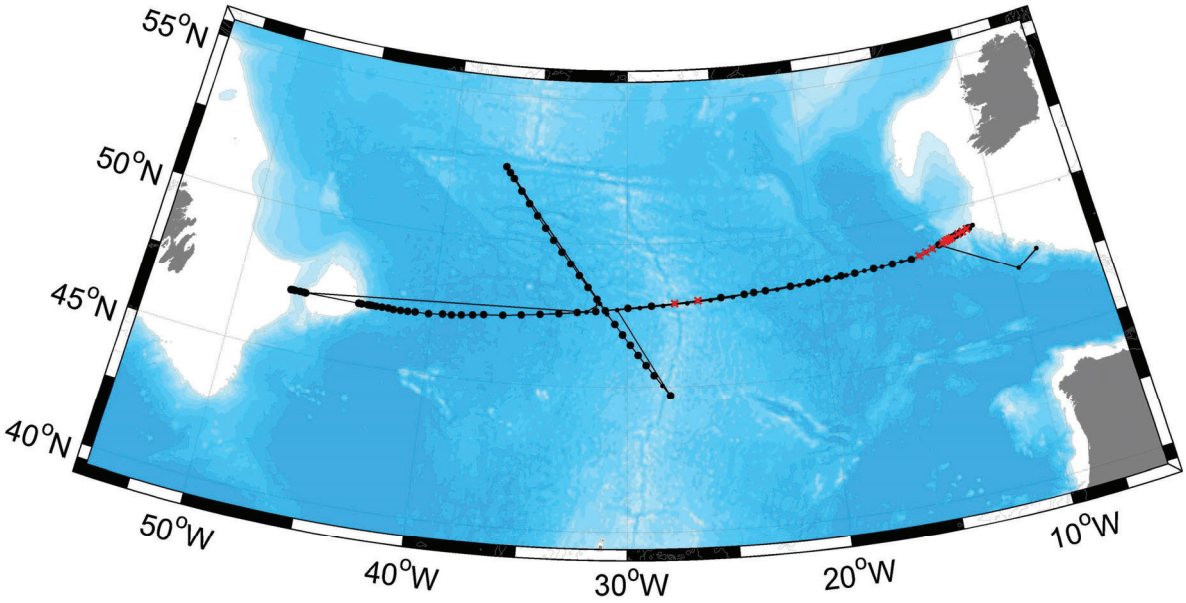

Fig. 5.8 Map showing the location of all stations (small black dots) along the cruise track (black line) and the 72 CFC-12 and SF_6 stations analysed on board (large black dots). Flame-sealed samples (see text below) are shown as red crosses. The bathymetry is shown in colours in steps of 500 dbar from 5000 dbar (dark blue) to dry land (in grey).

During this cruise we used an analytical technique for the simultaneous measurements of the trace gases sulphur hexafluoride (SF_6) and the chlorofluorocarbon component CFC-12 in seawater and air. The determination of these two compounds was accomplished by a purge and trap pre-treatment followed by gas-chromatographic (GC) separation on a capillary column and micro electron capture detection (micro-ECD). This system, with slight changes, was also used on previous cruises. The system is calibrated by analyzing several different volumes of a known standard gas. Additionally, the blank of the system was analyzed regularly. For details of the analysis see *Bulsiewicz et al.* (1998). Concentrations of CFC-12 in air and seawater are reported on SIO-98 scale while SF_6 concentrations are reported on the NOAA-2006 scale, both according to the used gas standard, which was prepared and calibrated at CMDL, Boulder, Colorado.

Water-samples from station #003/004 to #008/009 were collected into 230 ml glass ampoules from 10 l Niskin bottles. This water was at first transferred into a calibrated volume (i.e. a 150 ml volume) and then into a water purge chamber. We used this larger volume to address the expected low tracer concentrations in the deep East Atlantic basin. Later we changed the sample ampules to 200 ml and the calibrated volume to 113 ml.

After purging the water with purified nitrogen, the extracted gases were trapped on a 1/8" ID large *Porapak-Q* packed trap, cooled by liquid CO_2. Thermal desorption released the sample gases held in the trap, and they were further transferred onto a *MS5A* pre-column, where SF_6 and CFC-12 were separated from nitrous oxide and any other late eluting gases. The sample compounds were then refocused on a 1/16" ID *Porapak-Q* packed trap to refine their peaks in the chromatogram and to improve their detection. After thermal desorption the released gases were separated on an *Aluminia Bond/CFC 0.54mm ID x 3m* pre-column and an *Aluminia BOND/CFC 0.54 mm ID x 30m* main column. SF6 and CFC-12 are finally detected on a micro-ECD.

In total we collected 1035 water samples from 85 stations (Figs. 5.8, 5.9). On board we analysed 900 individual water-samples from 72 hydrographic stations along the 47°N section and parallel to the Mid-Atlantic Ridge (large black dots in the map in Fig 5.8). Additionally, we sampled flame-sealed water samples from 13 stations that were analysed later in the lab at the IUP Bremen (Fig. 5.8; see text below).

Based on the analysis of replicate water samples (39 or 4.5% of all samples), we estimated precisions < 1.0 % for both dissolved SF_6 and CFC-12 measurements obtained from the on-board analysis of measured samples. The overall accuracy is ~2.5% for SF_6 and ~1.5% for CFC-12.

The analysis of three air measurements gave the results listed in Table 5.4 and are in good agreement with the extrapolated air data obtained from the NOAA/ESRL halocarbons in situ program website, available at http://doi.org/10.7289/V5X0659V, see *Dutton et al.* (2017).

Tab. 5.4 Air measurements of CFC-12 and SF6 during cruise *M164* and air values adopted from *Dutton et al.* (2017) and extrapolated to July 2020.

	air measurement 1	air measurement 2	air measurement 3	from NOAA data, extrapolated
CFC-12 [ppt]	500.70	499.75	494.85	~ 496.5 ± 1.8
SF_6 [ppt]	10.38	10.38	10.43	~ 10.5 ± 0.1

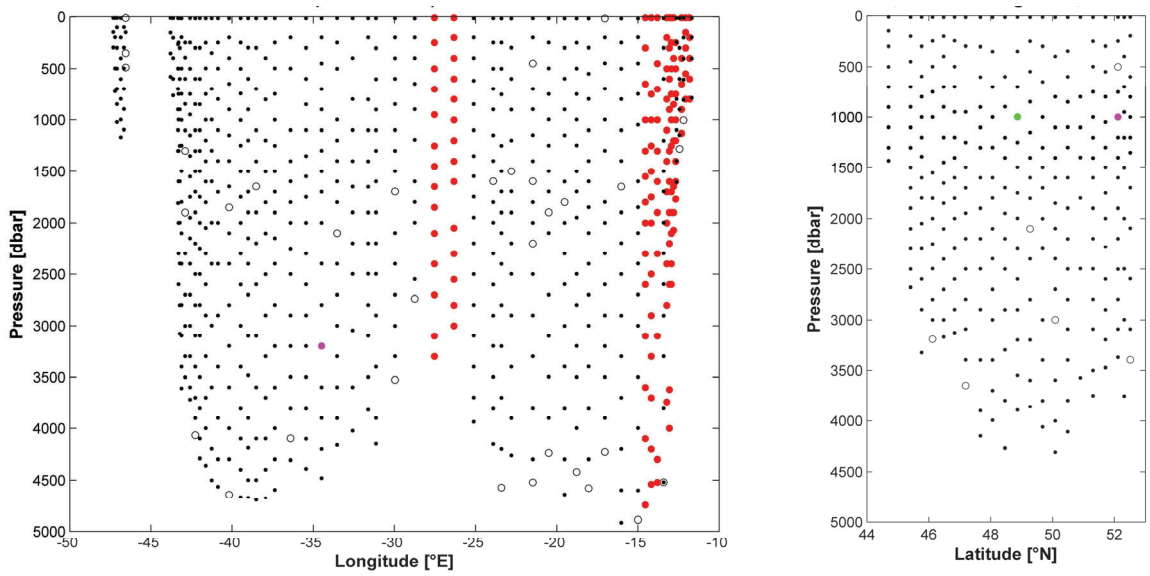

Fig. 5.9 *Vertical distribution of all 1035 CFC-12 and SF_6 measurements on 85 stations, separated into a zonal section along 47°/48°N (left) and a meridional section along the Mid-Atlantic Ridge (MAR, right). Black dots represent good measurements on board. Green are doubtful, and magenta are bad measurements. Black circles indicate 39 means of replicates. The red dots indicate the position of the flame-sealed samples.*

At the beginning of the cruise the performance of the micro-ECD detector was not satisfying. We observed a rising baseline and an unusual high noise level. These early measurements (stations #003/004 to #008/009) may have a larger uncertainty as the following ones. To improve the performance of the detector, we reduced the detector temperature. This reduced the noise level, but also the sensitivity of the detector. While adjusting the parameters of the GC/ECD system (stations #012/013 to #025/025), we collected water sampled into 200 ml glass ampoules that where flame-sealed after a tracer-free head space of purified nitrogen had been applied. These tracer samples were analysed later in the CFC-laboratory at the IUP Bremen.

Duo to an undetected leakage in the connection between the standard gas and the measurement system, we had lost all standard gas at station #038/038. We refilled the empty gas cylinder with atmospheric air, using an on-board compressor. On board, we preliminary calibrated that new standard gas against air samples and the known atmospheric tracer partial pressure (atmospheric

CFC-12 and SF_6 data from the NOAA/ESRL halocarbons in situ program; *Dutton et al.* (2017)). While preparing the new standard (stations #039/039 and #040/040) we sampled the water into glass ampoules that where flame-sealed and later on analysed in the CFC-laboratory at the IUP Bremen. The new standard was accurately re-calibrated in our home lab against a well known standard.

Finally, we had observed a significantly high water blank, particularly for CFC-12, which we could not reduce or interpret. We suspected this blank signal to influence also the water measurements, in a way that particularly CFC-12 measurements tended to be too high under certain circumstances. Hence, near the end of the cruise while on the way back to Emden, we carried out several test measurements, first, to understand the reason for this blank. Preliminary results of these test measurements indicated that a larger volume of the water purge chamber than the calibrated water volume tended to increase the blank, possibly due to remains of water in the un-rinsed top of the purge chamber. Second, we looked to find a correction for that blank and increased measurements. Due to the limited time at the end of the expedition, the detailed and careful analysis of these test measurements was carried out in the lab at IUP Bremen.

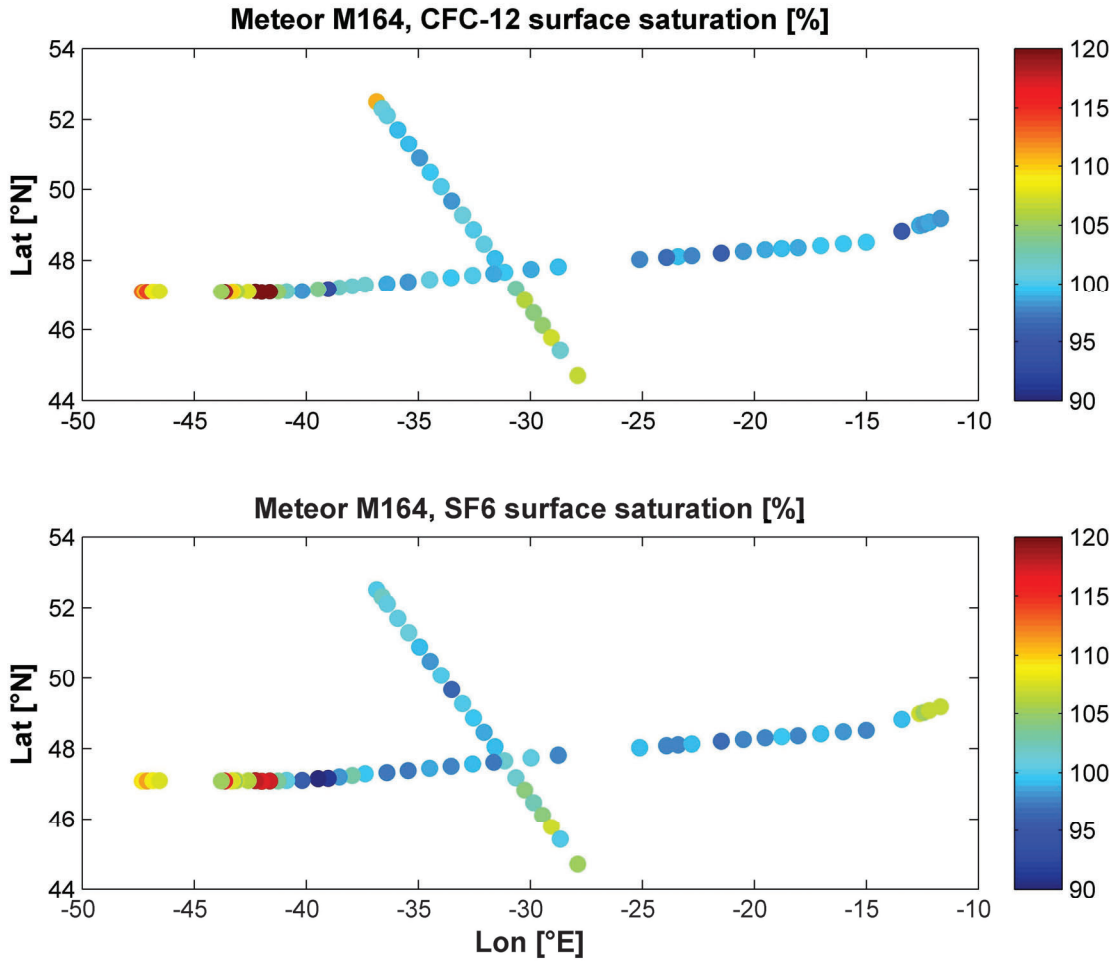

Fig. 5.10 Tracer saturations from measurements within the upper 20 dbar. Surface water tracer saturations range in the same order as in previous years.

Surface water saturations (upper 20 dbar, Figure 5.10) from the tracer measurements were usually slightly below 100% for both CFC-12 and SF_6 in the East Atlantic Basin and increased west of the Mid-Atlantic Ridge to values above 100%. Data shown here are preliminary due to re-calibration of the on board collected new standard.

5.3 Performance of Lowered Acoustic Doppler Current Profilers

(K. N. Wiegand, D. Kieke, C. Gapp, A. Hunkemöller, L. Krisztian, I. Leimann, J. Stiehler)

The Lowered Acoustic Doppler Current Profiler (LADCP) set-up in use during cruise *M164* consisted of two *Teledyne RD Instruments* (TRDI) *Workhorse Monitor* ADCPs, operating at 300 kHz that were attached to an *SBE32* carousel water sampler. To stabilize the water sampler with the additional weights of the ADCPs and the respective power supply, weights of about 300 kg in total were additionally mounted on the water sampler. The water sampler was typically lowered with a speed of 1.0 m/s and heaved with 1.2 m/s, decreasing the velocity in the upper and lower 100 meters of the water column. The ADCP instruments were configured to operate in a synchronized configuration with the downward-looking device mounted at the bottom of the water sampler triggering the upward-looking device mounted at its top. LADCP data were recorded on all CTD casts. In total, 126 CTD/LADCP casts were performed.

Prior to the cruise four ADCP devices to be used were verified and calibrated at the University of Bremen in Bremen, Germany, regarding the devices' internal compasses. Two instruments (s/n 7915 and 24522) were calibrated as downward-looking and two as upward-looking devices (s/n 1973 and 2161). During the cruise the instruments were powered by an external battery pack, which consisted of 35 commercial quality 1.5 V batteries lasting around 40 to 45 hours. These were assembled in a modified *Aanderaa* pressure housing. The ADCP system was configured to a ping rate of 1 Hz and 10 m depth cell size (bin length), the detailed individual instruments settings are listed in Table 5.5.

The processing of the raw data was done using two software toolboxes side by side. As a first approach the LADCP-toolbox for MATLAB, version 1.2.2, of the Department for Oceanography at the University of Bremen was used for immediate processing and inspection of the raw data from the combined instrument set-up. This software packages takes raw data of both, down- and upward-looking ADCPs into consideration as well as auxiliary data like measurement of time and pressure of the respective CTD casts. Vertical profiles of absolute oceanic velocities are determined from applying a shear and an inverse method *(Visbeck, 2002*) to the post-processing of the raw data. The latter incorporates velocities obtained from bottom tracking that is only available should the downward-looking LADCP device be close enough to the sea floor to detect it.

Tab. 5.5 Sequence of *Teledyne-RDI* commands used during cruise *M164* in order to program the LADCP instruments in a synchronized mode with required settings.

Downward-looking device	Upward-looking device
WM15	WM15
WV250	WV250
WN20	WN20
WS1000	WS1000
WF0	WF0
WB1	WB1
EZ0011101	EZ0011101
EX11111	EX11111
CF11101	CF11101
WP1	WP1
TP 00:01.00	TP 00:01.00
TE 00:00:01.00	TE 00:00:01.00
SM1	SM2
SA001	SA001
SW75	ST3600
CQ255	CQ255
CK	CK
CS	CS

Furthermore, the raw data were processed with the LDEO LADCP processing software, version IX.13 (*Thurnherr, 2018*), which provided the final version of the LADCP data set of cruise *M164*. This software estimated a shear solution and as well incorporated bottom track velocities. Vessel-mounted ADCP data for the upper part of the water column were incorporated to constrain the inverse solution of the resulting absolute velocity profiles. In particular, the data of the vessel-mounted ADCP system of type *Ocean Surveyor 75 kHz* were implemented to obtain a high vertical resolution of the upper boundary condition. Furthermore, the LDEO software processed GPS-derived latitudes and longitudes, time, and pressure data derived from the corresponding CTD cast (1 Hz and 1 dbar resolution, respectively) to estimate the location of the ADCP devices in the water column. In addition, it used calibrated CTD conductivity to correct for sound speed variations within the water column, and had tools implemented to remove any occurring data spikes.

Throughout the cruise, data from all LADCP casts were processed individually for both, the down- and upward looking devices (LDEO-toolbox only), and using raw data from both devices combined (both toolboxes). The final data set was obtained from combining the data of both instruments and with the mentioned auxiliary data (GPS, CTD, OS75) included and processing carried out with the LDEO-toolbox.

In the beginning of the cruise we installed a GPS antenna as close as possible to the point where the CTD is lowered into the water, and we fed respective GPS information obtained on the corresponding station (date, time, latitude, longitude; 24 Hz resolution) directly into the CTD raw data recording. During station/profile #001/002, #031/031, #037/037, #038/038 the GPS antenna lost contact with the satellites, so we had to incorporate the ship's GPS data afterwards. From station/profile #039/039 onwards we directly switched to the ship's GPS system. Furthermore, we regularly and automatically synchronized the internal clock of both data recording PC systems (CTD and LADCP) with the vessel's UTC time server to compensate for any clock drifts of the two PC systems. Experiences from a previous cruise had shown that PC clock drifts had occurred before, which had made the data processing regarding the synchronization of the LADCP and CTD data more complex.

As we experienced problems with the vessel's mechanical movebar, the station/profile #017/019 was aborted at about 250 dbar and was repeated as station/profile #021/021. During station/profile #100/098 *R/V METEOR* experienced a complete blackout when our water sampler with the mounted LADCPs was at a depth of approximately 15 meters, just returning from the deep. Since afterwards the storing of navigational positions failed, for station/profile #100/098 and #101/099, the vessel-mounted ADCP data that were incorporated into the LADCP processing were used with fixed position data.

The final version of the processed LADCP data set includes absolute ocean velocity (u, v, error velocity) on a depth grid resolved at 10 m. The *International Geomagnetic Reference Field 13* (IGRF13), valid in summer 2020, was used to infer the correct magnetic declination, i.e. the difference between magnetic and true bearings, at each station location and station time.

Throughout the cruise the LADCP system worked mostly flawless. During the first mounting of the LADCPs we figured a broken plastic screw on device s/n 1973 that held the cover plate for the LADCP's pressure sensor. The screw was exchanged, but nevertheless we decided to mount s/n 2161 as up-looking device. At station/profile #060/060 the processing software stated for the first time that beam 3 of the up-looking LADCP was apparently broken and the profile was calculated using a 3-beam solution in 28% of the time. This warning was repeated for the following station/profile #061/061 with a 3-beam solution in 33% of the time. The next warning occurred for station/profile #067/067 where no beam was broken according to the processing software but nevertheless a 3-beam solution was used in 33% of the time. Thus, we changed the up-looking device (before s/n 2161, afterwards s/n 1973). Tab. 5.6 lists the serial numbers of the devices in use at particular stations.

Tab. 5.6 Station and CTD/LADCP profile numbers of cruise *M164* and serial numbers of down- and upward-looking ADCP instruments.

M164 Station/Profile number	Serials number of downward-and upward-looking LADCP devices (# / #)
#001/001 - #067/067	24522 / 2161
#068/068 - #128/126	24522 / 1973

Throughout the cruise, the power consumption of the ADCP system was checked and the devices' run-time during each LADCP cast, from the wake-up to the powering-down of the devices, was monitored. Consequently, in total we used 7 battery sets equipped with fresh batteries. For the last battery set we used batteries that have already been used for tests of acoustic releases during station/profile #001/002. Individual battery cycle times ranged from 40 to 45 hours (Fig. 5.11). Overall, the power supply did not show any failures. One of the additional outputs of the LDEO software is a first guess battery voltage. As the software is not calibrated to the used devices we measured the battery voltage after each profile using a multimeter to compare the measured voltage to the given value of the software. After 4 battery cycles we found an empirical solution for the software to fit very well with our measured battery voltages (Fig. 5.11).

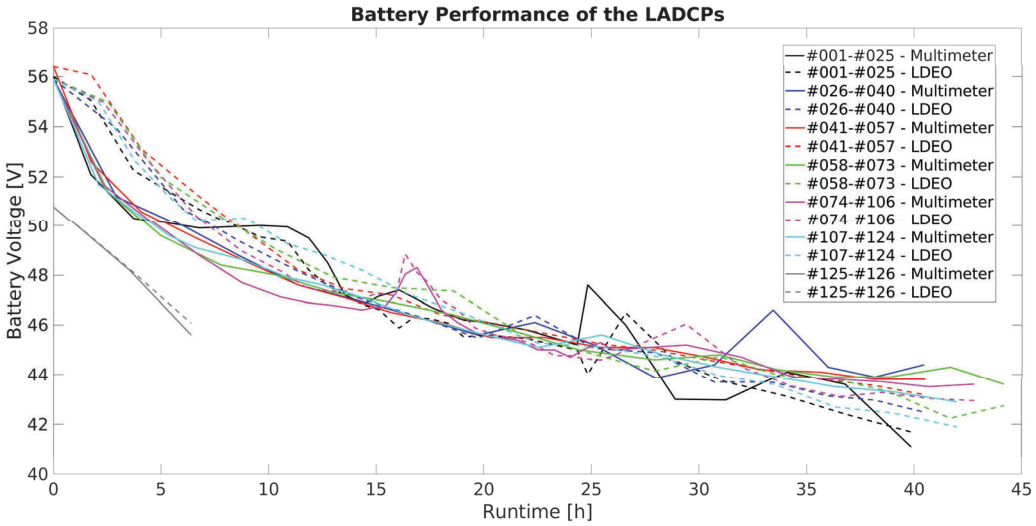

Fig. 5.11 Overview on the battery performance of the LADCP setup during cruise *M164*. Colors highlight the different battery cycles, solid lines are the measured battery voltage using a multimeter, dashed lines are the solution of the LDEO software, numbers in the legend refer to LADCP profile numbers.

During different stations/profiles we experienced larger differences in the weather conditions. The analysis of two stations/profiles with strong (#035/035, about 6-7 Bf) and weak (#039/039, about < 2 Bf) winds showed that there was no distinguishable difference in the data quality according to stronger winds. This was also due to the ship being very stable most of the time. Stronger movement of the ship during a station/profile induces movement of the water sampler with the two attached LADCP devices. Another factor is that during wind stirring and strong ship movements, air bubbles might be generated underneath the hull of the ship where the vessel-mounted ADCPs are installed. This may impact on the quality of the respective data incorporated into the LADCP processing. We did not observe such strong movements.

Another potential error source are strong currents itself. The higher the current velocity, the higher the forces that act on the water sampler. During previous cruises we observed that high current velocities often resulted in turns of the water sampler as it is not perfectly streamlined, and thus strong currents force the water sampler to rotate. This time we did not observe high numbers of rotations of the water sampler. Even at the station/profile #079/077, located directly in the core of the Deep Western Boundary Current with strong southward velocities, the water sampler did

not experience a single rotation (Fig. 5.12). To conclude, during cruise *M164* we did not observe strong ship movement due to stronger wind, and we also did not observe high numbers of rotations of the water sampler due to strong currents. Thus, the overall quality of the LADCP data was fine during the entire cruise.

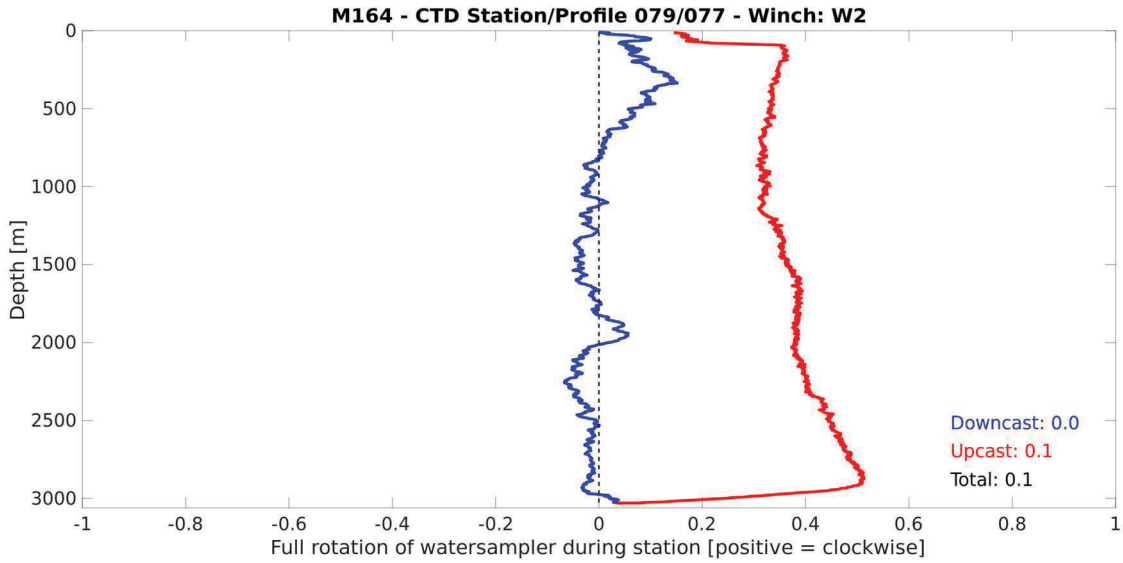

Fig. 5.12 Water sampler rotations during *M164* CTD station/profile #079/077. Downcast movement is shown in blue, upcast movement in red. Numbers describe total rotations of the water sampler (positive = clockwise).

5.4 Performance of Vessel-Mounted Acoustic Doppler Current Profilers

(J. Stiehler, I. Leimann)

Two Vessel-Mounted Acoustic Doppler Current Profilers (VMADCP) manufactured by *Teledyne RD Instruments* (TRDI) were used for continuous recording of single ping velocity data in the upper water column: a 75 kHz *Ocean Surveyor* (OS75) and a 38 kHz *Ocean Surveyor* (OS38), both with flat phased-array transducers. The 75 kHz OS was mounted into the hull of the ship, and the 38 kHz instrument was installed in the moon pool of the ship. Both OS instruments worked well throughout the cruise.

The OS38 was aligned to zero degrees (relative to the ship's centerline) in order to reduce interference with the OS75, which was aligned to 45°. Since the VMADCPs do not have any further built-in sensors, additional data on heading and tilt were obtained from the ship's *Seapath* system.

Data recording was carried out with the TRDI *VmDas* software, version 1.46. For the whole cruise, both ADCPs worked in narrow-band mode to provide maximum vertical coverage and sustain consistency with the existing data series obtained from previous cruises. Characteristic parameters for each device are listed in Tab. 5.7.

Tab. 5.7 Characteristics of the two VMADCPs of type 38 kHz Ocean Surveyor (OS) and 75 kHz Ocean Surveyor, operated during cruise *M164*.

	38 kHz OS	**75 kHz OS**
	narrow-band mode	**narrow-band mode**
Bin size [m]	32	8
Number of Bins	55	100
Blanking Distance [m]	16	4
Maximum Range [m]	1000-1500	600-700
Transducer Angle [°]	0	45
Transducer Depth [m]	6.615	6.945

The obtained raw data were processed using two different data processing toolboxes:

a) VMADCP-Toolbox OSSI for MATLAB, version 1.9, of the *GEOMAR Helmholtz Centre for Ocean Research Kiel*

b) CODAS (Common Ocean Data Access System) toolbox of the University of Hawaii, USA, running on *VirtualBox* (CODAS_bionic_64_1), version updated in April 2020.

Processing of VMADCP resulted in datasets of zonal and meridional current velocities, distributed over latitude, longitude, time, depth along the ship track. The processed data were stored in several output files in the native MATLAB format (*.mat, OSSI and CODAS) and netCDF format (CODAS) at temporal resolutions of 1 min (OSSI) and 1, 5, and 10 min (CODAS). Erroneous signals from the sea bottom were removed in the resulting data files for both devices.

The data recording started on the 25th of June 2020 at 07:30 UTC in the French EEZ. Recording stopped on the 29th of July 2020, 02:45 UTC in the French EEZ. The general operation of the two VMADCP devices was manually documented throughout the cruise in individual log files. Whenever a system was restarted, individual files were created and the file counter was automatically increased. During the mentioned data recording period, both VMADCPs were switched off and on several times due to various reasons, i.e. during PIES telemetry operations and mooring work, when low-noise acoustic environments were required.

During the processing of the VMADCP data, a water-track calibration was performed to determine phase and amplitude of the transducer misalignment. The amplitude scale factor and transducer orientation were calculated so as to minimize the root-mean-square differences between the estimated water velocity over the ground (using GPS navigation) before and after ship accelerations, including major turns as well as stopping on station and getting underway after a station. Respective adjustments are listed in Tab. 5.8.

Tab. 5.8 Calculated amplitude factors and misalignment angles for the two VMADCP systems, operated during cruise *M164*, using the OSSI and the CODAS processing toolboxes.

(OSSI/ CODAS)	38 kHz OS	75 kHz OS
Amplitude factor	1.0025 / 1.0006 (std: 0.0188)	1.0010 / 1.0005 (std: 0.0190)
Misalignment angle	0.0559° / 0.0005° (std: 0.4227)	-0.1702° / -0.0040° (std: 1.4468°)

The instruments have worked properly during the whole cruise, and the data are of good quality. However, the data need further additional post-cruise quality control and post-processing steps to obtain a final dataset, e.g. detailed inspection and manual editing of suspicious measurements.

Figure 5.13 shows examples of the current velocity recorded by the OS75 system along the cruise track. The strongest currents are located, as expected, in the western basin of the North Atlantic, like the northward North Atlantic Current (NAC) and its adjacent recirculation, or the Labrador Current in the Flemish Pass. When combining the current field with temperature information (Fig. 5.14), a general west-east and north-south temperature gradient becomes obvious. Currents on the Grand Banks are the coldest, as they originate in the northern Labrador Sea followed by the currents passing around Flemish Cap and currents at the Mid-Atlantic Ridge at about 52°N. The warmest currents are found in the West European Basin as well as in the Newfoundland Basin where warm temperatures indicate the presence of branches of the North Atlantic Current and its respective recirculation.

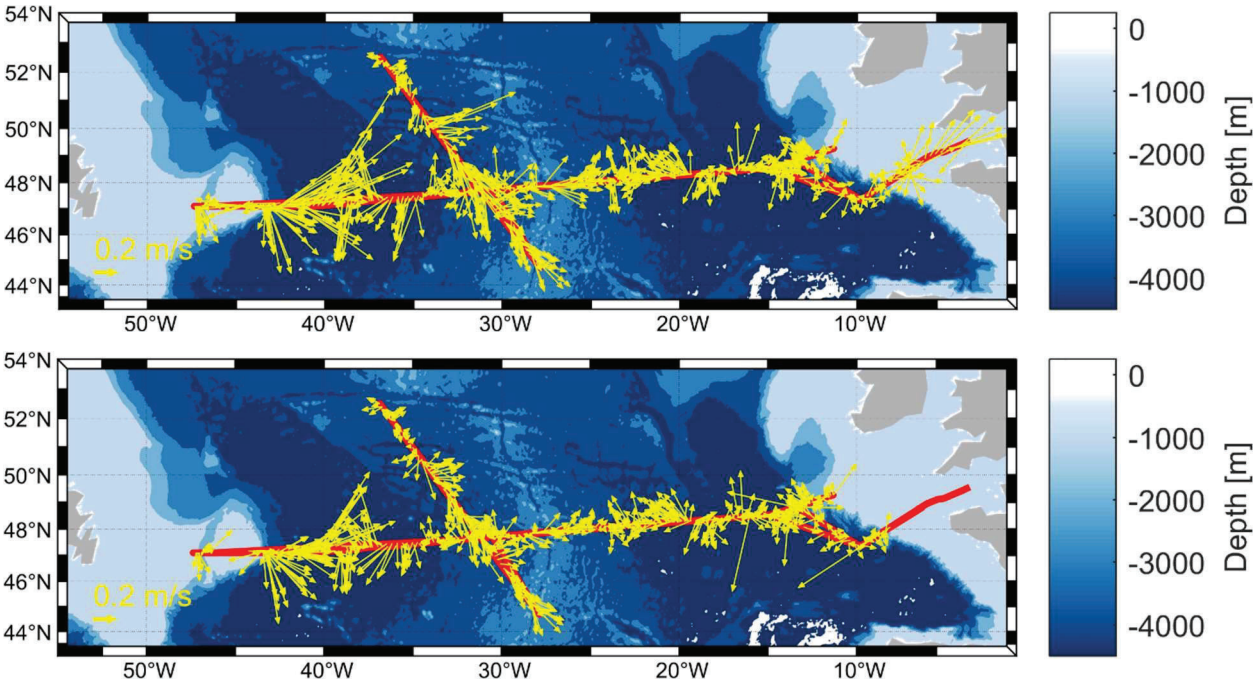

Fig. 5.13 Current velocities recorded along the cruise track (red) by the OS75 VMADCP, averaged over the upper 250 m layer (top) and for 250-750 m layer (bottom), cruise *M164*.

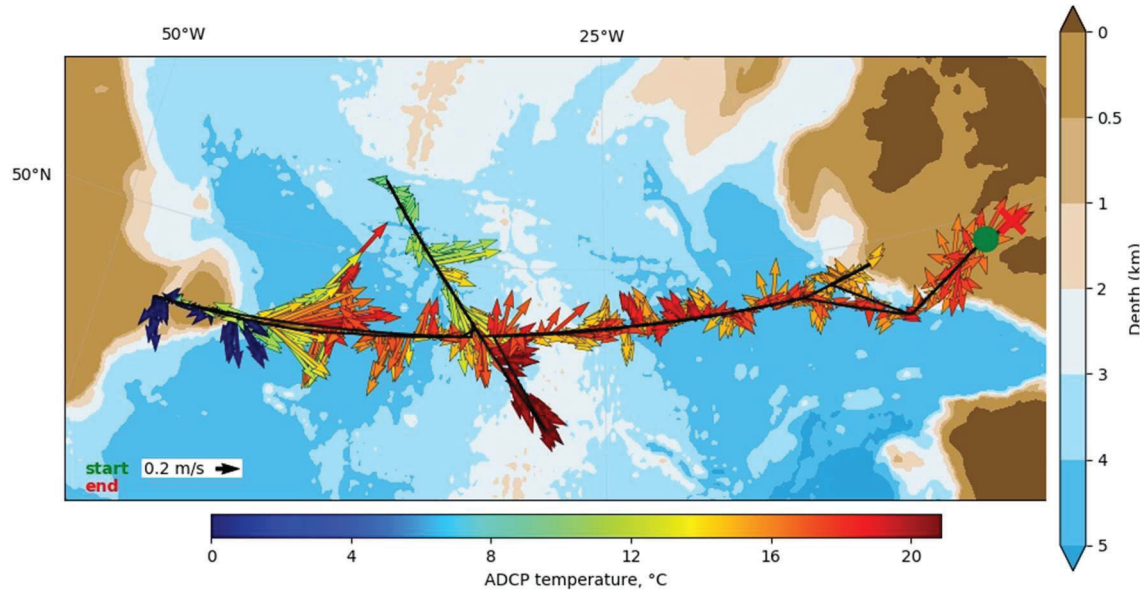

Fig. 5.14 Current velocities in the surface layers (upper 45 m) color-coded by temperature [°C] obtained from the OS75 transducer, cruise *M164*.

5.5 Inverted Echo-Sounders Equipped with Pressure Sensors (PIES)

(S. Wett, D. Kieke)

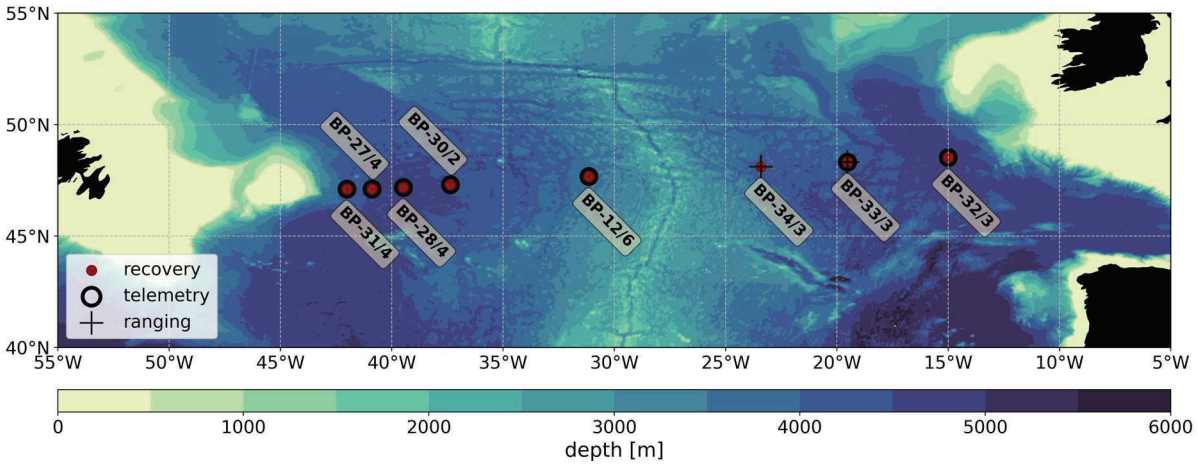

Fig. 5.15 PIES positions and operations along 47/48°N. Texts denote the names of the individual positions. Bathymetric data from *GEBCO Compilation Group* (2020).

5.5.1 Measurement Principle

PIES are moored devices used to determine oceanic volume transports over the course of a few years. They are inverted echo-sounders (IES) mounted to a metal frame, standing on the ocean floor, equipped with a pressure sensor. The metal frame serves as a bottom weight. The devices send a sound pulse and determine the round-trip travel time of this acoustic signal from the ocean bottom to the surface and back. All PIES were programmed to send pulses consisting of 12 individual pings at a frequency of 12 kHz, every 30 minutes. Since the speed of sound in seawater depends on temperature, salinity and pressure, the distribution of these hydrographic variables over the water column can be inferred by comparing the measured round-trip travel time to

estimates obtained from a number of reference CTD and Argo profiles. Simultaneously, the PIES measure the bottom pressure. The pressure sensors are known to be subject to instrument drift over time, which is why the PIES are typically installed for several years, as the drift becomes smaller with time. This is corrected in the post-cruise processing of the obtained data. In order to calculate the volume transports time series between a pair of instruments, the hydrographic information from the round-trip travel time and the pressure information need to be combined. The baroclinic volume transport from the hydrography and the barotropic volume transport from the pressure information add up to the total volume transport between two PIES.

In total we recovered eight PIES along 47°/48°N in the subpolar North Atlantic (Figure 5.15). Together with other instruments and repeated hydrographic ship sections they formed the *North Atlantic Changes* (NOAC) array that served to study the temporal and spatial evolution and relative importance of individual circulation branches forming relevant components of the Atlantic Meridional Overturning Circulation (AMOC) at 47°/48°N. Since cruise *M164* was the very last cruise funded through the BMBF-project *RACE*, we did not redeploy any PIES, and the basin-wide *NOAC* array was decommissioned by the end of the cruise.

5.5.2 Communication and Recovery

Ship-based communication with the PIES when they are installed in the water is possible via acoustic telemetry. Using a hydrophone and a deck unit (8-channel unit of type *Benthos DS-7000*), the PIES can receive a number of predefined commands and answer to these. Since the hydrophone installed on the hydraulic extension unit of *R/V Meteor* was out of order, we had to use our own portable hydrophone for the duration of the whole cruise. This is a hydrophone attached to a rope and equipped with an additional weight, which we veered approximately 25 meters into the water. It is more prone to detecting noise from the surface layer than the ship's hydrophone because it is moved by the waves and dragged by currents. However, in most cases the quality of the acoustic communication with the instruments was good.

Usually, after a PIES is deployed, ranging is performed. That means that the ship navigates around the drop-off position whereby we constantly measure the travel time of a ping sent at fixed intervals by the PIES (and thus the relative distance between the ship and the PIES) with a hydrophone. This is done in order to triangulate the exact geographical position and the depth of the device. Knowing the exact position of the device yields more accurate volume transports. For two instruments that we recovered, this procedure could not be done right after the deployment in 2019, so we performed the ranging before the recovery of the devices in these two cases.

The small amount of data actually stored on the device allows to remotely read out the data, measured by the PIES, as daily averages via acoustic telemetry. When receiving the respective command, the PIES sends its data as encoded acoustic signals on different frequencies. This way the data can be obtained in reduced temporal resolution before recovering the device. This reduces the risk of losing data in case the device cannot be recovered. For a decent quality of the acoustic telemetry the noise in the water needs to be reduced to a minimum, meaning all sound emitting devices need to be switched off and the ship should preferably hold its position without using the propellers or bow-thruster. Furthermore, wind, waves, bubbles in the water and marine mammals such as whales and dolphins can produce noise which is not controllable but might interfere with

the acoustic telemetry. In total, the data from seven of the eight PIES that were recovered was read out before recovery via acoustic telemetry. From these seven devices the data was therefore saved as daily averages. The acoustic telemetry cannot be performed between 23:30 UTC and midnight UTC because in that period the PIES conducts its own calculations. Thus, whenever we could not finish the telemetry before 23:30 UTC we interrupted it before and resumed after midnight.

After successful acoustic telemetry the PIES can be recovered by sending the acoustic release command. The PIES detaches from its metal frame and ascends to the surface while constantly pinging. These status pings make it possible to anticipate the time when the device will be at the surface. Compared to moorings with many floatation elements, the PIES are rather small and are mounted in a white shell which makes it hard to spot them in the water during daylight. Thus, they are equipped with a bright flashing light, making recovery in the night a lot easier than during the day. Additionally, once the device is at the surface, a radio transmitter indicates the PIES' position relative to the ship.

Before or after each PIES' recovery we measured a CTD profile at the position of the device. These add to the database of CTD profiles used to convert the travel time measured by the PIES into hydrographic information. Furthermore, measuring the current velocity over the water column before recovering the instruments makes it easier to anticipate the drift of the device during its ascend to the surface. Knowing the direction in which the device will probably drift while coming to the surface makes it possible to position the ship in a way that the PIES is recovered easiest.

After the recovery of each PIES, the data stored on the internal memory card was read out on board. This ensures that the data recorded by the instruments is saved in full temporal resolution. Afterwards the devices were cleaned and prepared for the transport back to Bremen.

5.5.3 PIES Activities During Cruise *M164*

A chronological summary of all PIES activities during cruise *M164* is provided in Table 5.9. We reached the PIES position *BP-32/3* on June 30 after finishing the work on the eastern boundary moorings (*EB-1* and *EB-3*). We successfully performed the acoustic telemetry of this first instrument with only a small amount of noise. The signal from the released PIES was rather noisy and the expected shape of the status pings was hardly visible, possibly due to the weather conditions and the hydrophone moving under the rolling ship. However, we successfully recovered the PIES eventually.

On the 2nd of July 2020 we reached the PIES position *BP-33/3*. When this device was deployed in May 2019 ranging could not be performed. Thus, we conducted the ranging in order to calculate the exact position and depth of the device. Afterwards we read out the data of the last year via acoustic telemetry. The noise level of the telemetry was low and only a few days were missing in the transmitted data. The telemetry was intentionally interrupted at 23:30 UTC to account for the PIES' own calculation time. After midnight the telemetry was resumed. Subsequently, we released the PIES. This time, as well as for all following devices, the shape of the status pings during the ascend of the instrument was clearly visible and the PIES was successfully recovered.

The last of the eastern PIES was *BP-34/3*, deployed in May 2019 and not read out since then. With daylight approaching, when we reached the position on the 4th of July 2020, we decided not to release the PIES but to perform the acoustic telemetry. Though, we got answers from the instrument, indicating that it understood the commands, we did not receive any valid data via acoustic telemetry. This was possibly due to the harsh weather conditions with strong winds (7-8 Bf), which produced a lot of noise in the water column. We decided to leave this position for now and recover the device on our transit back to Emden, Germany.

BP-12/6 is one of the oldest Bremen PIES positions. The device here was deployed in May 2018 and last read out in May 2019. We reached this position on the 6th of June 2020 and successfully read out the device via acoustic telemetry. After waiting for the night, we released the PIES and successfully recovered it.

BP-30/2 is the easternmost PIES position in the western basin (see Fig. 5.15). The PIES was deployed here in April 2016 and last read out in June 2019. We reached the position on the 12th of June 2020. This time many whales and dolphins were around the ship causing a lot of noise in the data of our acoustic telemetry. We received a telemetry signal, but a lot of data points were missing. After waiting for the darkness to recover the device, the whales and dolphins were still around, but did not interfere with this operation and so we successfully recovered the PIES.

In the night of the 13th of July 2020, we reached the next PIES position in the western basin, *BP-28/4*. This device was deployed here in May 2018 and was last read out in June 2019. We read out the new data via acoustic telemetry. Again, we intentionally interrupted the telemetry before 23:30 UTC to account for the PIES' calculation period and resumed after midnight UTC before successfully recovering the PIES.

On the 14th of July 2020, we reached the PIES position *BP-27/4*. The acoustic telemetry was performed successfully, and for the recovery we had to wait for the night. Thus, we did a CTD profile in between and then returned to the PIES position to successfully recover the device.

Finally, on the 15th of July 2020, we reached the westernmost PIES position *BP-31/4*. With this device we were also able to perform the acoustic telemetry and successfully recover it after waiting for the night and doing another CTD profile in between. After recovering the device, we tried to contact again PIES *BP-31/3* that had been deployed on this position in May 2018 but did not respond to any command in June 2019. Unfortunately, we were again not able to establish any communication with the device, which meant that it was either no longer at its location or that severe electronic failures caused it to malfunction. As a consequence, this device was given up.

On our way back to Emden, Germany, we arrived at the position *BP-34/3* again on the 24th of July 2020 to range and recover the PIES in a second attempt. This time the weather conditions were still not optimal but better than during our first attempt. Since the ranging of this device had not been carried out after the deployment we successfully located the device via ranging. Afterwards, with daylight approaching, we did not do acoustic telemetry of *BP-34/3*, but successfully recovered the device and read out the data on board afterwards. Thus, from this device

we only have the high-resolution data stored on the device's memory card and not the daily averages from the acoustic telemetry.

All data obtained from the PIES, either via telemetry or through instrument recovery (see Tab. 5.9), will be analyzed as part of the post-cruise analysis.

Tab. 5.9 Overview on activities related to inverted echo-sounders equipped with pressure sensors (PIES) carried out during cruise *M164*.

M164 Station	PIES ID	s/n	Latitude	Longitude	Depth [m]	Ranging Date/Time	Telemetry Date/Time	Recovery Date/Time	CTD #
26-1	BP 32/3	075	48°31.09'N	15°00.10'W	4784	---	30 Jun 2020 19:40–23:20	30 Jun–01 Jul 2020 23:06–00:50	26
31-2	BP 33/3	240	48°18.57'N	19°31.42'W	4532	02 Jul 2020 18:54–20:07	02 Jul 2020 20:47–00:54	03 Jul 2020 01:05–02:36	31
35-1	BP 34/3	362	48°06.47'N	23°25.09'W	4489	---	04 Jul 2020 04:18–05:35 telemetry failed	---	35
43-2	BP 12/6	271	47°39.79'N	31°08.66'W	4094	---	06 Jul 2020 16:34–20:02	06–07 Jul 2020 22:31–00:29	43
63-2	BP 30/2	235	47°18.06'N	37°21.70'W	4539	---	12 Jul 2020 18:17 – 21:44	12–13 Jul 2020 23:00–00:41	63
67-2	BP 28/4	272	47°10.21'N	39°28.70'W	4605	---	13-14 Jul 2020 20:30–01:32	14 Jul 20120 02:13 – 03:58	67
69-2	BP 27/4	302	47°06.11'N	40°53.04'W	4499	---	14 Jul 2020 14:55–18:19	14–15 Jul 2020 23:56–01:48	69
72-2	BP 31/4	201	47°05.90'N	42°01.02'W	4222	---	15 Jul 2020 13:12–16:14	15–16 Jul 2020 22:47–00:25	72
74-1	BP 31/3	303	47°05.17'N	42°00.77'W	4246	---	16 Jul 2020 00:50–01:28 communication failed	---	72
119-2	BP 34/3	362	48°06.47'N	23°25.09'W	4489	24 Jul 2020 22:30-22:59	---	24-25 Jul 2020 23:23-00:59	119

5.6 Mooring Activities

(M. Köllner, A. Schneehorst, T. Svensson, D. Kieke)

Mooring work carried out during cruise *M164* consisted of recovering three and redeploying two deep-sea moorings. Two of them, *EB-1* and *EB-3* were located on the crest of Goban Spur, a topographic obstacle at the Irish continental slope (Figs. 5.16, 5.17). The third mooring, *BM-22*, was located on the eastern flank of Flemish Cap, another topographic obstacle on the western side of the Atlantic Ocean (Figs. 5.18, 5.19). All moorings served to capture the strength and the variability in the strength of the eastern and western boundary currents (EBC and WBC). While the EBC basically transfers waters of subtropical origin to the north, the WBC exports subpolar water towards the south. Together with the PIES installed in the deep basins along 47°/48°N the moorings have formed the long-term deep-sea observing system NOAC ("North Atlantic Changes"). NOAC has been maintained by the University of Bremen and the German Federal Maritime and Hydrographic Agency (BSH), Hamburg, and has served to quantify the circulation and relevant components of the Atlantic Meridional Overturning Circulation (AMOC) at 47°/48°N. By the end of the cruise, the NOAC array had not been continued as all PIES and the western mooring had to be de-installed due to the scientific project and funding period coming to an end. The two *EB* moorings, now both maintained by BSH, however, were continued and redeployed at their original position.

5.6.1 Mooring Activities at the Eastern Boundary

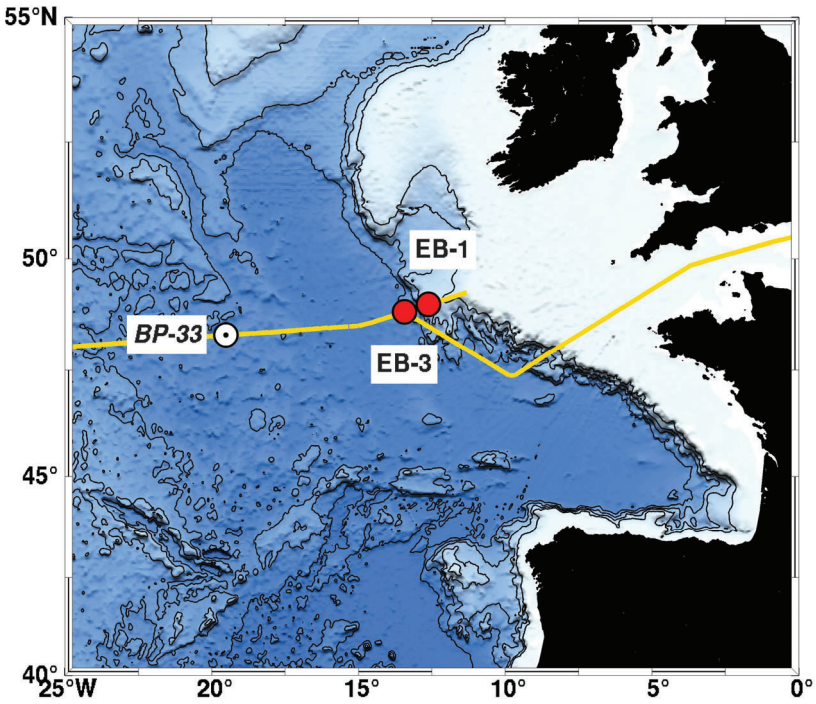

Fig. 5.16 Location of the deep-sea moorings *EB-1* and *EB-3* (red markers) recovered and reinstalled during cruise *M164* along the crest of Goban Spur off the Irish shelf break. Dark yellow lines denote the cruise track, the white circle highlights the easternmost PIES-location, *BP-32*.

Tab. 5.10 Overview of mooring activities carried out at Goban Spur during cruise *M164*. All times are given as UTC. The top buoy of the moorings was equipped with radio beacons, flashers, flags, and *Iridium* or *Argos* beacons.

M164-Station	Mooring ID	Latitude	Longitude	Depth [m]	Recovery Date/Time	Deployment Date/Time	CTD Profile
4-1	EB-1/4	49°00.03'N	12°37.02'W	1553	27 Jun 2020 17:00 – 22:05	---	5
19-1	EB-1/5	49°00.22'N	12°37.01'W	1550	---	29 Jun 2020 16:00 – 17:20	5
3-2	EB-3/4	48°49.98'N	13°26.03'W	4454	27 Jun 2020 07:32 – 13:40	---	4
18-1	EB-3/5	48°50.45'N	13°25.30'W	4450	---	29 Jun 2020 07:54 – 12:38	4

The aim of the boundary current array at Goban Spur is to monitor variability in transports and water mass properties associated with the northward spreading of subtropical waters along the eastern boundary. Together with the information about the water mass variability at the MAR from moorings deployed between 2009 and 2015 within the projects *Nordatlantik* and *RACE* it is aimed at assessing the sources of water mass variations being advected into the Nordic Seas and the Arctic Ocean. The mooring activities at the eastern boundary during *M164* consisted of recovering and redeploying moorings *EB-1* and *EB-3* deployed during *MSM83* in 2019. Until 2020, mooring *EB-1* was maintained by the University of Bremen, while mooring *EB-3* was maintained by the Federal Maritime and Hydrographic Agency (BSH), Hamburg. In 2020, BSH deployed both *EB*-moorings under its sole responsibility.

The *EB-1/4* mooring was recovered during the afternoon of June 27, 2020. Mooring activity started at 17:00 UTC with the communication to the acoustic release. Release commands were sent to the releases using a deck unit of type *IxSea Oceano TT-300B* (s/n 296) and a hydrophone with 20 m cable length. At 17:12 UTC the surfacing of the top element of the mooring was observed. Out of two radio beacons (*Novatech* s/n V01-026, *Xeos* s/n 498), one Iridium transmitter (*Xeos* s/n 237, HB-4) and a flasher (*Novatech* s/n V09-046), all installed in the top buoy of the mooring, only the flasher and one radio beacon (V09-046) worked reliably, the latter despite a heavily bent antenna. These two devices were equipped with commercial alkaline D-cells. Post-recovery inspection of the remaining devices showed that at least one Lithium battery per device was power-drained. During the recovery operation one of the mooring ropes got stuck somewhere underneath the front part of the ship's hull, the reason for this 'accident' being unknown. As a consequence, the respective rope had to be cut. As all floatation packages could be identified as still floating at the sea surface, nevertheless, the entire mooring could be completely recovered. At 22:05 UTC all parts of the mooring were successfully recovered. All instruments of the mooring were in good shape and without any damage. As in previous years however, all mooring ropes with lengths > 50m showed several cuts of unknown origin. Of all installed instruments, the *Teledyne RDI LongRanger* ADCP (s/n 5691) and two *SBE-37 MicroCAT*s (s/n 3026, 8900) collected data during the full length of the deployment period, and all collected data are usable.

Unfortunately, the two current meters of type *Nortek Aquadopp* (s/n 8425, 9932) did not record any data.

Mooring *EB-1/5* was deployed again on June 29, 2020 in the eastern boundary at Goban Spur at a water depth of 1500 m, with the top element of the mooring at 700 m depth to prevent it from possible fishing activities within the area. All instruments (two current meters of type *Nortek Aquadopp*, one *Teledyne RDI LongRanger* ADCP, three *SBE-37 MicroCAT*s, one *NKE* thermistor and two *RBR Duet T.D.* temperature-depth recorders) were mounted as planned. The top-buoy of the mooring was equipped with a *Sercel BASM800 Argos* beacon, a *Xeos XMB-11K* radio beacon and a *LongRanger* ADCP operating at 75 kHz. The head-buoy went into water at 16:00 UTC. The anchor was slipped at 17:16 UTC. The sinking of the top-buoy was observed at 17:20 UTC.

The *EB-3/4* mooring was recovered during the early morning of June 27, 2020. Mooring activity started at 07:32 UTC with establishing the communication to the acoustic releases. Release commands were sent to the release using the *TT801* deck unit (s/n 446) and a hydrophone with 30 m cable length. The release command was sent several times without any recognition of a response of the release by the deck unit. At 07:49 UTC the mooring was spotted at the surface. The radio beacon did not give any signal due to the orientation of the top-buoy keeping the beacon under water. The *Sercel Argos BASM 800* transmitter worked reliable. At 13:40 UTC, all parts of the mooring were successfully recovered. All instruments and other elements of the mooring were in good shape and without any damage. All instruments collected data during the full length of the deployment period. All data are usable. Preliminary results of the pressure time series indicated that the mooring was standing upright in the water column, two larger sinking events of the instruments in June 2019 and May/June 2020 could be observed.

Mooring *EB-3/5* was redeployed on June 29, 2020 in the eastern boundary at Goban Spur at a water depth of 4450 m, with the top element of the mooring at 500 m depth to prevent it from possible fishing activities within the area. All instruments (six current meters of type *AADI Seaguard*, two current meters of type *Nortek Aquadopp*, one *Teledyne RDI LongRanger* ADCP, 12 *SBE 37-SM MicroCAT*s, eight *NKE* thermistors and one *RBR Duet T.D.* temperature-depth recorders) were mounted as planned. The top-buoy of the mooring was equipped with a *Sercel BASM800 Argos* beacon, a *Xeos XMB-11K* radio beacon and a *LongRanger* ADCP. The top-buoy went into water at 07:45 UTC. The anchor was slipped at 12:12 UTC. The sinking of the buoy was observed at 12:39 UTC.

The NKE thermistors have temperature and pressure sensors that measure in a five-minute sampling interval. The temperature accuracy is ±0.05 °C in a 0 °C/20 °C range with a maximum resolution of 0.01 °C. The pressure sensor has a precision of 12 m (0.3 %) and a resolution of 1.2 m.

AADI Aanderaa Recording Current Meters (*Seaguards*) were programmed to measure velocity, direction, temperature, and pressure (optional) in a 60 minutes sampling interval. The accuracy of the temperature sensor is ±0.03°C, of the optional pressure sensor ±0.5 % of the full range, the resolution of the compass is 0.35° and its accuracy ±5°, and the precision of the speed sensor is ±1 cm/s.

SBE (*Sea-Bird Electronics*) *37-SM MicroCATs* were programmed to measure the temperature, conductivity, and pressure (optional) in a five-minute sampling interval. The accuracy for the temperature sensor is ±0.002 °C, for the conductivity sensor ±0.0003 S/m and 0.1 % of full-scale range for the optional pressure sensor.

The *Teledyne RDI LongRanger 75kHz ADCP* was programmed to measure velocity and direction up-looking in 16 m bins in up to 500 m distance to the instrument in a 30 min sampling interval. Additionally, the *LongRanger* measures pressure and temperature at its moored depth in the same interval. The accuracy of the temperature sensor is ±0.4 °C, of the pressure sensor ±0.25 % of the full range, the resolution of the compass is 0.01 ° and its accuracy ±2 °, and the precision of the speed sensor is ±1%.

Nortek Aquadopps were programmed to measure velocity, direction, temperature (embedded in head), and pressure in a 30 minutes sampling interval. The accuracy of the temperature sensor is ±0.1 °C, of the pressure sensor ±0.5 % of the full range, the resolution of the compass is 0.1 ° and its accuracy ±2 °, and the precision of the speed sensor is ±1% of the measured value (up to 1.5 cm/s).

RBR duet T.D. recorders measured temperature and pressure in a five-minute sampling interval. The temperature accuracy is ±0.002 °C. The pressure sensor has a precision of 3 m (0.05 %).

The *Argos* beacon transmits positional information every 90 seconds when it is on the surface. Under water the beacon sits in a stand-by (underwater) mode. The radio beacon transmits at a pre-programmed frequency as soon as it reaches the surface and can therefore be located using a direction-finding device. Under water it enters into a sleeping mode.

The acoustic releases (*Oceano* from *Ixblue*) were successfully tested in the laboratory. Prior to deployment, both releases were tested at 2700 m depth during station #002/002. All releases were tested with the *TT801* deck unit (s/n 446) and a hydrophone with 30 m cable. Three acoustic releases were programmed to respond to a frequency of 12 kHz, while one other release was programmed to respond to a frequency of 22 kHz. All releases responded to the diagnostic mode and to the release command and were open when they came back on deck.

On station #002/003, one *Aquadopp* (sampling interval 6 s), 13 *MicroCAT*s (sampling interval 6 s) and ten *NKE* recorders (sampling interval 6 s), all destined for the new deployment of mooring *EB-3/5*, were attached to the CTD/water sampler unit and brought to a maximum pressure of 3500 dbar. On station #016/018, two *MicroCAT*s (sampling interval 6 s), and three *RBR Loggers* (sampling interval 6 s) were attached to the CTD/water sampler unit and brought to a maximum pressure of 2090 dbar. On station #067/067, all *MicroCAT*s and *NKE*s recovered from moorings *EB-1/4* and *EB-3/4* were attached to the CTD/water sampler unit and brought to a maximum pressure of 4600 dbar. During the upcast of these three stations, the CTD/water sampler system was stopped four times at different pressure levels for 10 min each. These data were investigated to estimate any noticeable offset between the instruments and the calibrated CTD data. Most of the instruments measured within their proposed uncertainty ranges, see Tabs. 5.11 to 5.15.

Tab. 5.11 Mean offsets regarding temperature, conductivity and pressure (optional) between individual *MicroCAT* recorders and CTD data of station #067/067.

Sensor	Serial number	Temperature offset x10^{-3} [°C]	Conductivity offset x10^{-3} [mS/cm]	Pressure offset [dbar]	Deployed in EB1-2019/2020
SBE 37-SM	3026	3.3 ± 0.6	-0.1 ± 0.3	19.3 ± 0.3	x
SBE 37-SM	8900	-0.6 ± 0.8	-2.5 ± 0.8	---	x

Tab. 5.12 Mean offsets regarding temperature, conductivity and pressure (optional) between individual *MicroCAT* recorders and CTD data of station #002/003 and #067/067.

Sensor	Serial number	Temperature offset x10^{-3} [°C]	Conductivity offset x10^{-3} [mS/cm]	Pressure offset [dbar]	Deployed in *EB-3/4*, 2019/2020	Deployed in *EB*, 2020/2021
SBE 37-SM	14835	+3.0 ± 0.8	+1.2 ± 0.8	---	x	---
SBE 37-SM	14836	-1.6 ± 0.3	+0.3 ± 1.1	---	---	*EB-3/5*
SBE 37-SM	14837	+3.2 ± 1.0	-0.7 ± 0.7	---	x	---
SBE 37-SM	14838	+ 0.1 ± 1.3	-1.5 ± 2.2	---	---	*EB-3/5*
SBE 37-SM	14839	-2.5 ± 3.4	-0.3 ± 4.0	---	---	*EB-3/5*
SBE 37-SM	15158	+2.4 ± 1.4	+2.3 ± 1.3	+5.3 ± 0.7	x	---
SBE 37-SM	15159	+2.4 ± 1.0	-0.2 ± 1.0	+4.5 ± 0.8	x	---
SBE 37-SM	15160	+0.9 ± 3.2	-0.2 ± 4.0	+3.2 ± 0.8	---	*EB-3/5*
SBE 37-SM	15161	+1.2 ± 1.0	-4.4 ± 1.0	+4.0 ± 0.4	x	---
SBE 37-SM	15162	+2.2 ± 0.6	-2.8 ± 0.4	+4.3 ± 0.5	x	---
SBE 37-SM	15709	-1.0 ± 1.9	-3.3 ± 1.9	-2.7 ± 2.9	---	*EB-3/5*
SBE 37-SM	15710	+3.8 ± 1.4	-3.9 ± 1.3	-3.1 ± 1.3	x	---
SBE 37-SM	15711	+2.6 ± 2.3	-3.2 ± 2.5	-0.6 ± 1.2	x	*EB-3/5*
SBE 37-SM	20257	+0.9 ± 0.8	1.7 ± 0.7	-0.9 ± 0.9	x	*EB-3/5*
SBE 37-SM	20258	-2.3 ± 1.1	-1.9 ± 1.1	-2.2 ± 2.8	---	*EB-3/5*
SBE 37-SM	20259	-2.1 ± 1.5	-1.2 ± 1.9	-1.8 ± 2.2	---	*EB-3/5*
SBE 37-SM	20675	-1.3 ± 2.1	-6.9 ± 2.4	-1.6 ± 3.2	---	*EB-3/5*
SBE 37-SM	21501	+0.8 ± 1.9	-1.0 ± 2.6	-1.4 ± 2.5	---	*EB-3/5*
SBE 37-SM	21502	+0.1 ± 2.6	-2.7 ± 3.6	-0.4 ± 2.1	---	*EB-3/5*
SBE 37-SM	21506	-2.3 ± 1.6	-7.0 ± 2.8	-1.0 ± 2.2	---	*EB-1/5*
SBE 37-SM	21507	-1.8 ± 2.6	-18.3 ± 5.2	-0.4 ± 2.2	---	*EB-1/5*
SBE 37-SM	21510	-1.8 ± 0.4	-25.3 ± 3.9	-0.7 ± 2.3	---	*EB-1/5*

Tab. 5.13 Mean temperature offsets between individual *NKE* recorders and calibrated CTD data of station #002/003 and #067/067.

Sensor	Serial number	Temperature offset x10^{-2} [°C]	Pressure offset [dbar]	Deployed in *EB-3/4* 2019/2020	Deployed in *EB* 2020/2021
NKE SP2T4000-SI	36005	-2.1 ± 0.4	+18.1 ± 12.3	x	---
NKE SP2T4000-SI	36006	+1.1 ± 0.3	+16.7 ± 12.3	x	---
NKE SP2T4000-SI	36007	-6.7 ± 0.5	+15.8 ± 11.8	x	---
NKE SP2T4000-SI	36008	-0.5 ± 0.1	+16.9 ± 12.0	x	---
NKE SP2T4000-SI	36009	-0.7 ± 0.2	+18.6 ± 12.5	x	---
NKE SP2T4000-SI	36010	+0.1 ± 0.8	+9.8 ± 8.3	---	*EB-3/5*
NKE SP2T4000-SI	36011	-0.8 ± 1.6	+11.3 ± 9.5	---	---
NKE SP2T4000-SI	36012	-0.8 ± 0.6	+13.1 ± 9.1	---	---
NKE SP2T4000-SI	36049	+2.3 ± 0.7	+10.9 ± 8.9	---	*EB-3/5*
NKE SP2T4000-SI	36050	-1.7 ± 0.3	+19.3 ± 12.3	x	---
NKE SP2T4000-SI	36051	-1.4 ± 0.2	+16.7 ± 11.0	x	---
NKE SP2T4000-SI	36052	-1.1 ± 1.3	+11.3 ± 8.2	---	*EB-3/5*
NKE SP2T4000-SI	36053	+1.2 ± 0.4	---	---	---
NKE SP2T4000-SI	36054	-0.9 ± 0.4	+19.8 ± 11.7	x	---
NKE SP2T4000-SI	37001	+2.1 ± 0.4	+11.3 ± 9.1	---	*EB-3/5*
NKE SP2T4000-SI	37002	-1.6 ± 0.9	+12.5 ± 9.1	---	*EB-3/5*
NKE SP2T4000-SI	37003	-0.3 ± 0.2	+23.6 ± 13.9	x	---
NKE SP2T4000-SI	37004	-1.9 ± 0.1	+15.6 ± 12.9	x	---
NKE SP2T4000-SI	37005	-1.2 ± 0.3	+15.0 ± 9.6	---	*EB-3/5*
NKE SP2T4000-SI	37006	-1.2 ± 1.0	+13.2 ± 9.6	---	*EB-1/5*

Tab. 5.14 Mean temperature offsets between individual *RBR logger* and CTD data of station #016/018.

Sensor	Serial number	Temperature offset x10^{-3} [°C]	Pressure offset [dbar]	Deployed in *EB-3/4* 2019/2020	Deployed in *EB* 2020/2021
RBR Logger	95514	-1.3 ± 0.8	-0.93 ± 0.90	x	*EB-1/5*
RBR Logger	95520	-1.5 ± 1.3	+0.77 ± 0.49	x	*EB-1/5*
RBR Logger	95521	-2.0 ± 0.8	+1.08 ± 0.56	x	*EB-3/5*

Tab. 5.15 Mean temperature and pressure offsets between individual *Nortek Aquadopp* and CTD data of station #002/003.

Sensor	Serial number	Temperature offset x10^{-2} [°C]	Pressure offset [dbar]	Deployed in *EB-3/4* 2019/2020	Deployed in *EB-3/5* 2020/2021
Nortek Aquadopp	15602	-3.7 ± 10.9	21.1 ± 2.4	x	x

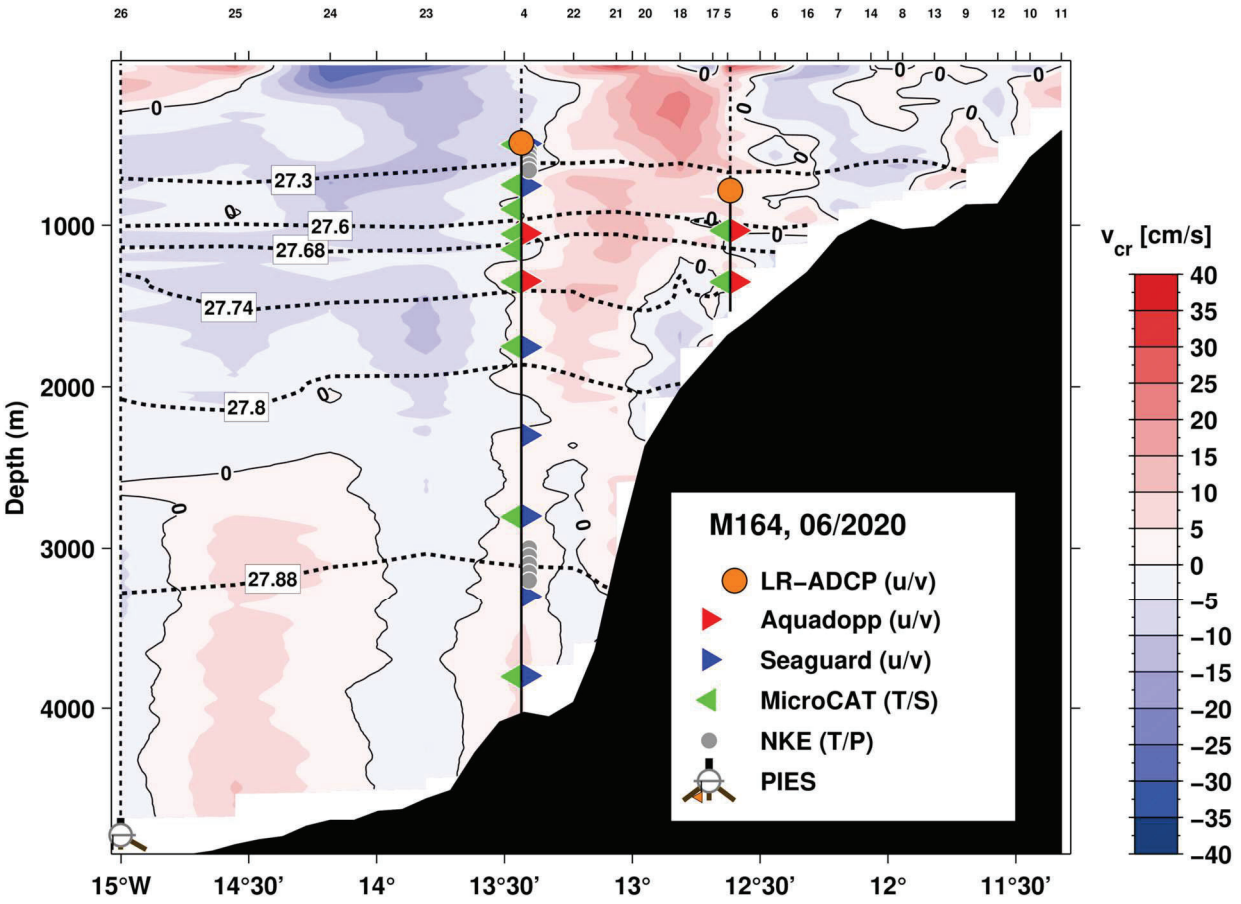

Fig. 5.17 Detided current velocity normal to the cruise track as shown in Fig. 5.16 and design of the eastern component of the NOAC mooring array recovered along the crest of Goban Spur, cruise *M164*.

5.6.2 Mooring Activities at the Western Boundary

Mooring activities at the western boundary of the North Atlantic focused on the recovery of the remaining deep-sea mooring *BM-22*, which was installed on the eastern flank of Flemish Cap in early summer 2019 (cruise *MSM83*). Mooring *BM-22* covered the slope core of the Deep Western Boundary Current (DWBC) and was recovered but not redeployed. Figures 5.18 and 5.19 highlight the location and the general design of the recovered mooring, while Table 5.16 summarizes details on the respective mooring activities carried out during cruise *M164*.

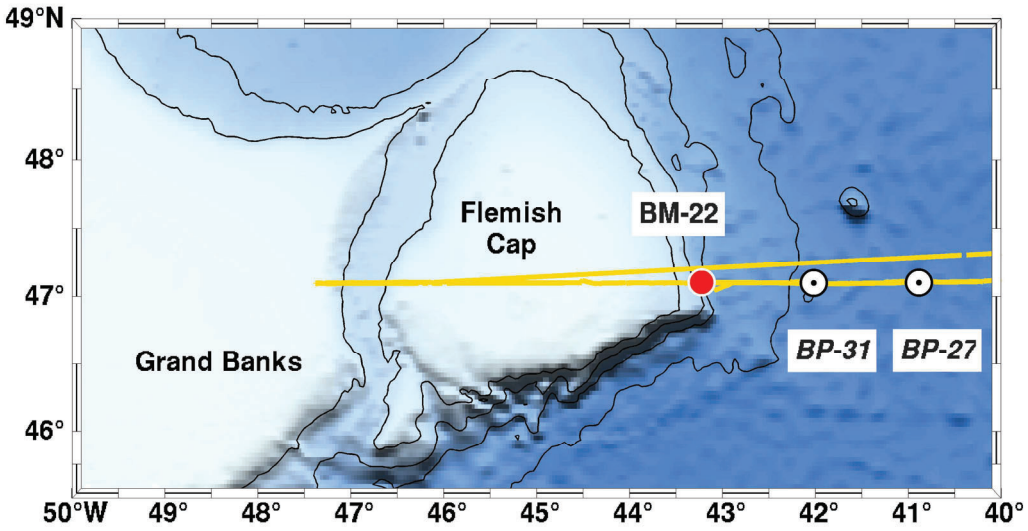

Fig. 5.18 Location of the deep-sea mooring *BM-22* (red dot), installed in the slope part of the western boundary current (WBC) east of the topographic obstacle Flemish Cap. Dark yellow lines denote the cruise track, the white circles highlight the westernmost PIES-locations, *BP-31* and *BP-27*. The mooring was successfully recovered during cruise *M164* but not redeployed.

Tab. 5.16 Overview activities carried out to the east of Flemish Cap, western North Atlantic, and related to mooring *BM-22*, cruise *M164*. All times are given as UTC. The top buoy of the mooring was equipped with radio beacons, flashers, flags, and Iridium beacons.

M164-Station	Mooring ID	Latitude	Longitude	Depth [m]	Recovery Date/Time	Deployment Date/Time	CTD Profile
76-1	BM-22/10	47°06.19'N	43°13.37'W	3048	16 Jul 2020 09:11 – 15:29	---	77

Mooring *BM-22/10* was recovered on July 16, 2020, in general at fairly well weather and sea state conditions. A large-scale field of prevalent sea fog, however, had a strong impact on the range of visibility, decreasing it to a few hundred meters only. As the sea fog was predicted to prevail over the coming days, and as the top buoy of the mooring was equipped with radio, flasher and Iridium beacons, the release command was sent at 09:16 UTC despite the fog using a deck unit of type *Oceano TT-300B* (s/n 296). The top buoy was expected to be detected at the surface only

minutes after sending the release commands. However, none of the attached radio or Iridium beacons provided any information that helped to locate the mooring. As the visibility range was below 500 m, we set course to follow a snake-like search pattern with focus on the region located to the southeast-to-east of the actual mooring deployment position. Evaluation of available ship-based measurements regarding strength and direction of the near-surface wind and ocean currents pointed to this as the most likely region, the mooring would tend to drift to. About three hours after sending the release command, the fog field lightened up, and the floatation bodies could be indeed successfully spotted at the surface in this region. Afterwards, the mooring was completely recovered.

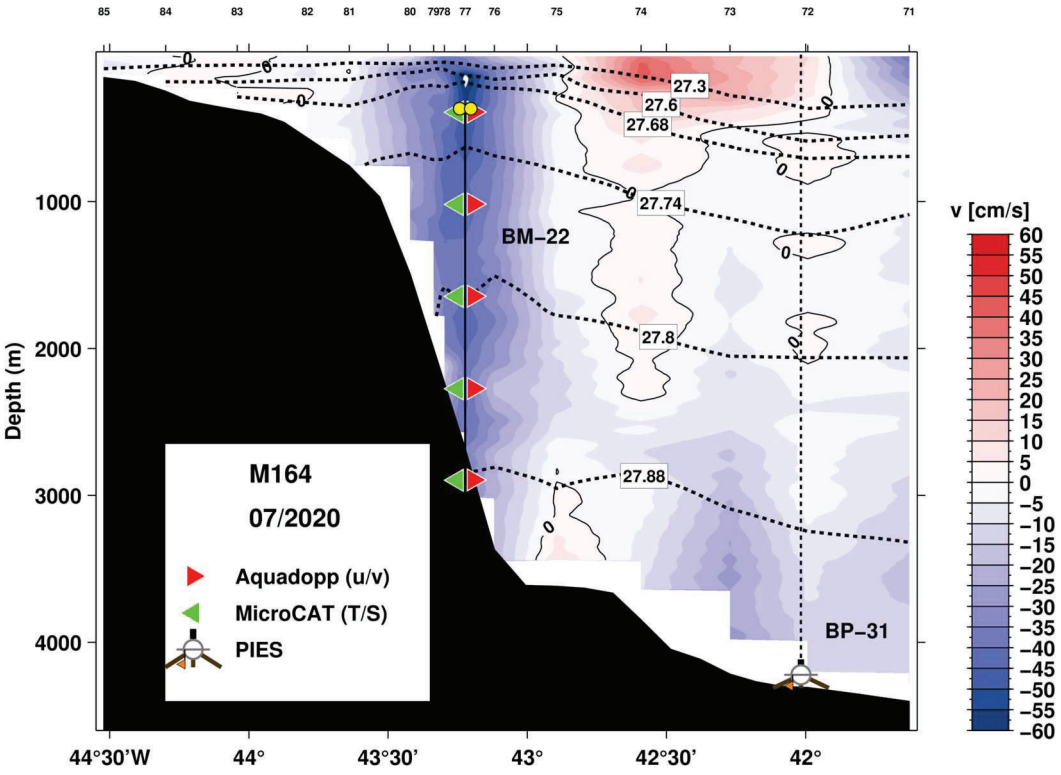

Fig. 5.19 Meridional velocity along to the cruise track as shown in Fig. 5.18 and location and design of the westernmost component of the NOAC mooring array, mooring *BM-22*, recovered on the eastern flank of Flemish Cap during cruise *M164*.

Like in previous deployment periods, mooring *BM-22/10* was located in the centre of the DWBC within its so-called slope core and almost covered the entire water column. Scientific devices were spread between 350 and 2850 m (Fig. 5.19). Core devices of the recovered mooring comprised five current meters of type *Nortek Aquadopp DW* (s/n 8538, 8542, 13020, 13024, 13032), five temperature-conductivity recorders of type *SBE 37-SM MicroCAT C-T* (s/n 7279, 8895, 8898, 8899, 8901), a single acoustic release of type *IxSea Oceano 2500-S Universal* (s/n 1874), *Dyneema* ropes of varying thickness (8 and 12 mm), and shackles and connecting rings made of titanium. The top buoy carried a flag, two VHF radio beacons of type *Xeos XMB-11k* (s/n 138, 168), an LED flasher of type *Xeos XMF-11k* (s/n 211), and a subsurface *Iridium* satellite beacon of type *MetOcean iCBN-3* (s/n F02-017). Only the flasher had worked correctly during recovery. Post-deployment inspection showed that one radio (s/n 168) and the *Iridium* beacon both

showed at least one empty lithium battery. The radio beacon s/n 138 revealed water intrusions that had damaged the lowermost battery. Radio signals and messages from the Iridium beacon could thus not be successfully received.

Data recorded by the *MicroCATs* were recovered using the *SBE* software *SeaTermV2*, version 2.6.1.12. *Aquadopp* data was recovered using the *Nortek* software *Aquadopp Deep Water*, version 1.40.14. All recovered data did not show any notable flaws.

On station #102/100, all *MicroCAT* and *Aquadopp* recorders obtained from the mooring *BM-22/10* were attached to the CTD/water sampler unit and brought to a maximum pressure of 4148 dbar. During the upcast, the system was stopped four times at different pressure levels for 10 min each. The sampling interval of the *MicroCAT* devices was 6 s. These data were investigated to estimate any noticeable offset between the instruments and the calibrated CTD data. The *Aquadopp* current meters were similarly attached to the water sampler frame and were set to a sampling interval of 1 sec. Tables 5.17 and 5.18 list the determined mean offsets between the devices and calibrated CTD data of these stations.

Tab. 5.17 Summary of mean offsets determined for the temperature and conductivity sensors of the *SBE MicroCAT* devices installed in the mooring *BM-22* and compared against calibrated CTD data from cruise *M164*, CTD station #102/100.

Sensor	Serial number	Temperature offset ΔT × 10^{-3} [°C]	Conductivity offset ΔC × 10^{-3} [mS/cm]	CTD #
SBE 37-SM	7279	+2.3 ± 0.4	+13.8 ± 0.5	102/100
SBE 37-SM	8895	+0.0 ± 0.3	-2.7 ± 0.5	102/100
SBE 37-SM	8898	+1.4 ± 0.3	-2.8 ± 0.5	102/100
SBE 37-SM	8899	+0.3 ± 0.3	+4.2 ± 0.5	102/100
SBE 37-SM	8901	+1.8 ± 0.3	+4.0 ± 0.4	102/100

Tab. 5.18 Summary of mean offsets determined for the temperature and pressure sensors of the *Nortek Aquadopp DW* devices installed in the mooring *BM-22/10* and compared against calibrated CTD data from cruise *M164*, CTD station #102/100.

Sensor	AQD serial number	Temperature offset ΔT [°C]	Pressure offset ΔP [dbar]	CTD #
Aquadopp DW	8538	+0.12 ± 0.02	−13.9 ± 6.1	102/100
Aquadopp DW	8542	-0.08 ± 0.01	−16.3 ± 6.0	102/100
Aquadopp DW	13020	−0.27 ± 0.02	+11.7 ± 3.3	102/100
Aquadopp DW	13024	−0.26 ± 0.02	+10.7 ± 3.2	102/100
Aquadopp DW	13032	−0.38 ± 0.02	+9.8 ± 2.5	102/100

5.7 Deployment of Profiling Floats

(A. Schneehorst)

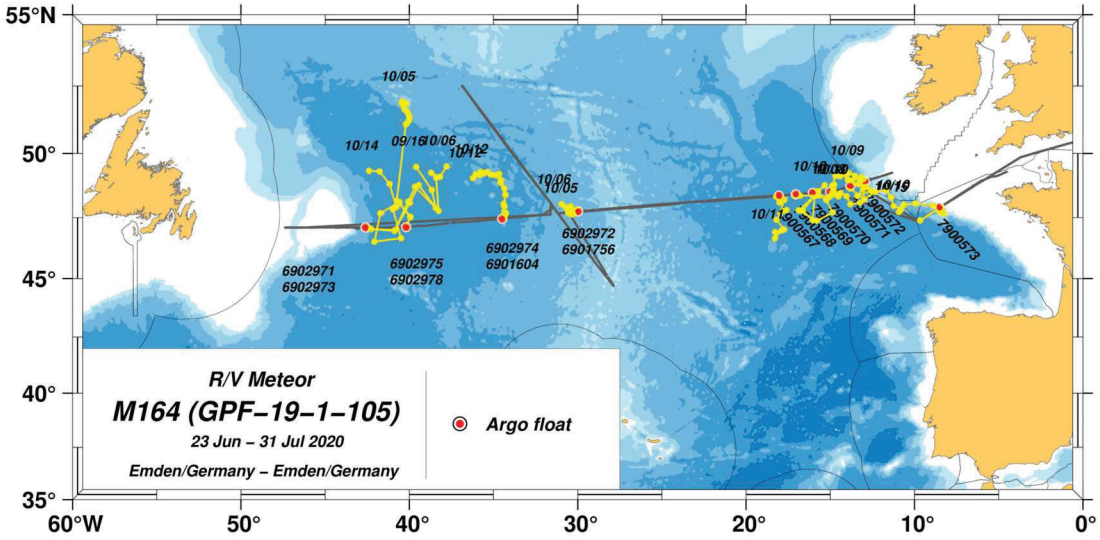

Fig. 5.20 Locations of Argo floats deployed during cruise *M164*. Given numbers denote WMO float identifiers. Grey lines highlight the cruise track. Small text labels denote month and day of the most recent profile and float location (yellow markers connected by yellow lines), status as of October 15, 2020.

During the cruise *M164*, fifteen profiling floats were deployed. All float deployments contribute to the international Argo program. The deployments of seven floats were carried out on behalf of the BSH (Germany), and the deployment of eight floats were carried out on behalf of Ifremer (France). Argo is an international program that collects information from inside the ocean using a fleet of robotic instruments that drift with the ocean currents and move up and down between the surface and predefined water levels. Each instrument (float) spends almost all its life time below the surface. The collected data describe the temperature and salinity of the water, and some of the floats measure oxygen in addition. The main reason for collecting these data is to help us understand the oceans' role in earth's climate and so be able to make improved estimates of how it will change in the future. Two different types of profiling floats were deployed along the cruise track. *Arvor I*, equipped with Iridium satellite telemetry, provide salinity, temperature and pressure profiles. The respective floats were programmed to drift for 9 days at a fixed pressure of 1000 dbar, their profiling pressure depth is 2000 dbar. *Deep Arvor*, also equipped with Iridium satellite telemetry, provide salinity, temperature, pressure and oxygen data. These floats were programmed to drift for 9 days at a pressure of 2750 dbar, and the profiling depth was set to 4000 dbar. All deployed floats were equipped with pressure, temperature and conductivity sensors manufactured by *SBE*. Both float types are manufactured by *NKE Instrumentation*. From their predefined parking depths, the floats are supposed to descend down to their profiling depths before rising and collecting vertical profiles of pressure, temperature, and conductivity, on their way to the surface. The deep floats collect additionally oxygen data. At the surface the floats transmit the collected data via satellite towards the land station. Having finished their transmission the floats sink again, and the profile cycle starts all over again. The cycle interval is 10 days in total. The expected lifetime for the *Arvor I* floats is 330 cycles (9 years) and 120 cycles (3 years) for the

Deep Arvor floats. Data are freely available usually within 24 hours after collection from the Argo data centers, like the *Coriolis* data centre at *Ifremer*, France (https://dataselection.euro-argo.eu/).

Tab. 5.19 Overview on Argo float deployments carried out during cruise *M164*.

M164-CTD-Station	Float s/n	WMO ID	Latitude	Longitude	Deployment Date/Time	CTD #
1-3	AI2600-20DE012	7900573	47°53.717'N	08°30.666'W	26 Jun 2020 02:09	1
20-2	AI2600-20DE006	7900572	48°55.524'N	12°57.113'W	29 Jun 2020 20:19	20
23-2	AI2600-20DE005	7900571	48°44.910'N	13°48.555'W	30 Jun 2020 07:30	23
26-3	AI2600-20DE004	7900570	48°31.088'N	15°00.092'W	01 Jul 2020 03:54	26
27-2	AI2600-20DE003	7900569	48°28.688'N	16°02.141'W	01 Jul 2020 11:36	27
28-2	AI2600-20DE002	7900568	48°25.356'N	17°02.343'W	01 Jul 2020 18:17	28
29-2	AI2600-20DE001	7900567	48°22.170'N	18°02.919'W	02 Jul 2020 01:09	29
42-2	AD2700-18FR011	6902972	47°44.917'N	29°57.998'W	06 Jul 2020 09:18	42
42-3	OIN-015-ARDP-01	6901756	47°44.893'N	29°58.032'W	06 Jul 2020 09:18	42
60-2	AD2700-18FR013	6902974	47°27.285’N	34°29.662’W	12 Jul 2020 00:41	60
60-2	OIN-015-ARDP-08	6901604	47°27.285’N	34°29.662’W	12 Jul 2020 00:41	60
68-2	AD2700-18FR014	6902975	47°06.833’N	40°11.064’W	14 Jul 2020 09:22	68
68-3	AD2700-18FR017	6902978	47°06.810’N	40°11.084’W	14 Jul 2020 09:23	68
75-2	AD2700-18FR010	6902971	47°06.025’N	42°35.499’W	16 Jul 2020 06:05	74
75-2	AD2700-18FR012	6902973	47°06.025’N	42°35.499’W	16 Jul 2020 06:05	74

Figure 5.20 highlights the location of float deployments carried out during cruise *M164* and surface locations since then, while Figure 5.21 shows respective temperature and salinity profiles available as of October 15, 2020.

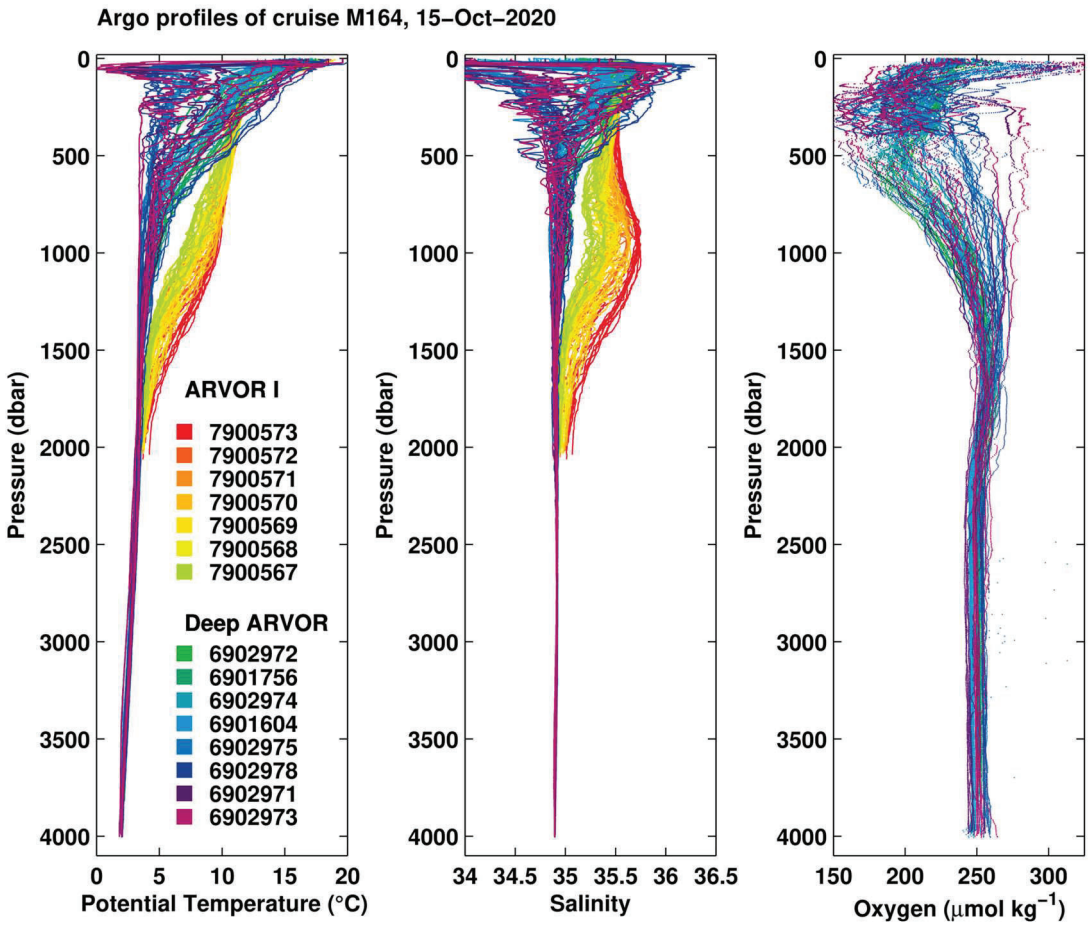

Fig. 5.21 Temperature (left), salinity (middle), and oxygen (right, only Deep Argo floats) profiles of all Argo floats deployed during cruise *M164*, status as of October 15, 2020. Colours and text labels refer to the individual float distinguished by their WMO float identifiers, compare Figure 5.20 and Table 5.19.

5.8 Underway Measurements

(D. Kieke, R. Steinfeldt)

A large variety of underway measurements were carried out during cruise *M164*. Among the acquired data of interest were navigational information, near surface hydrography (temperature, conductivity, and thus salinity) measured by the vessel's thermosalinograph (TSG) or the weather station operated by the German Weather Service (DWD) (water temperature only), as well as further meteorological parameters recorded by the meteorological sensors of the weather station.

With the exception of navigational and meteorological data that was recorded from the beginning of the cruise on, recording of additional underway data started on June 25 at 07:30 UTC, and ended on July 29 at 02:45 UTC. All data was logged in time steps of 1 second by the vessel's Davis-Ship system (DSHIP). All underway data relevant to this cruise was exported from the database on a daily basis and converted into MATLAB-readable netCDF-files. Water depths

measured by the deep-water multi-beam echo-sounder system *EM122* were recorded throughout the cruise. Data from selected CTD profiles were fed into the system to allow for a correction of the sound velocity. Apart from this, the data was not processed any further. The unprocessed raw data of the multi-beam system were sent to the bathymetric data centre at BSH at the end of the cruise. There, they are stored and curated under the data set number M164.202006. For the purpose of the cruise, water depths were noted on hydrographic stations.

5.8.1 Thermosalinograph Data

(R. Steinfeldt)

The thermosalinograph (TSG) system provides underway measurements of temperature, conductivity, and salinity. The water inlet connections are in the bulbous bow, several meters below the water line. The system is doubled, one is located at the port (P) and one at the starboard (ST) side. External temperature sensors (*SBE38*) are located directly at the entry point and measure the temperature of the water outside. The *SBE21* sensors further inside measure conductivity and temperature to infer the salinity of the sea water. Both systems are normally operating simultaneously.

In order to check the quality of the TSG data, they are compared with the CTD measurements. Therefore, the TSG values from the time when a CTD station started and the CTD data from the upper 4 dbar of that station (the CTD values form 0-4 dbar are identical) have been used.

The salinity of both TSG systems shows significant offsets towards the CTD data of -0.027 (port side) and -0.069 (starboard side) respectively, see Table 5.20. and Fig. 5.22. The salinity offset shows variations over time, and the difference between the port and starboard system slightly decreases. The salinity differences also depend on temperature (Fig. 5.22), with higher salinity offsets at larger temperatures. A linear regression of the salinity residuals towards time and temperature reveals that this temperature dependence is the main reason for the apparent temporal fluctuations of the TSG salinity offsets. Around days 190 and 200, when the offset is relatively small, *R/V METEOR* was at the northern (day ~190) and western (day ~200) end of the cruise track, where the surface temperatures (SSTs) where relatively cold, around 10°C. The last CTD stations, on the other hand, showed SSTs around 20°C, accompanied with the greatest bias of the TSG salinity. The recommended correction for the TSG salinities is given in Table 5.21. An additional temporal correction term is only necessary for the portside system.

The (external) TSG temperatures agree quite well with the SSTs measured by the CTD. For both TSG systems (Fig. 5.23), the offset is of the order of the accuracy of the TSG temperature sensors (0.01°C). In addition, the standard deviation of the temperature difference between TSG and CTD is about one magnitude larger (around 0.1°C, see Table 5.20). Thus, we do not recommend any correction for the TSG temperatures.

Tab. 5.20 Differences between TSG values and CTD data.

TSG Container	Salinity [psu]		Temperature [°C]
	TSG – CTD uncalibrated	TSG – CTD calibrated	TSG - CTD
Port	-0.027 ± 0.040	0.000 ± 0.027	0.008 ± 0.099
Starboard	-0.069 ± 0.075	0.000 ± 0.026	0.011 ± 0.099

Tab. 5.21 Calibration string for TSG salinity data of cruise *M164*.

TSG system	TSG Salinity Calibration String
Port	S_{corr} = S – 1.826996552356832e-01 + 8.233294540039610e-04*time + 3.351428239234803e-03*temperature
Starboard	S_{corr} = S + 1.651667619296530e-02 + 3.561472055556627e-03*temperature

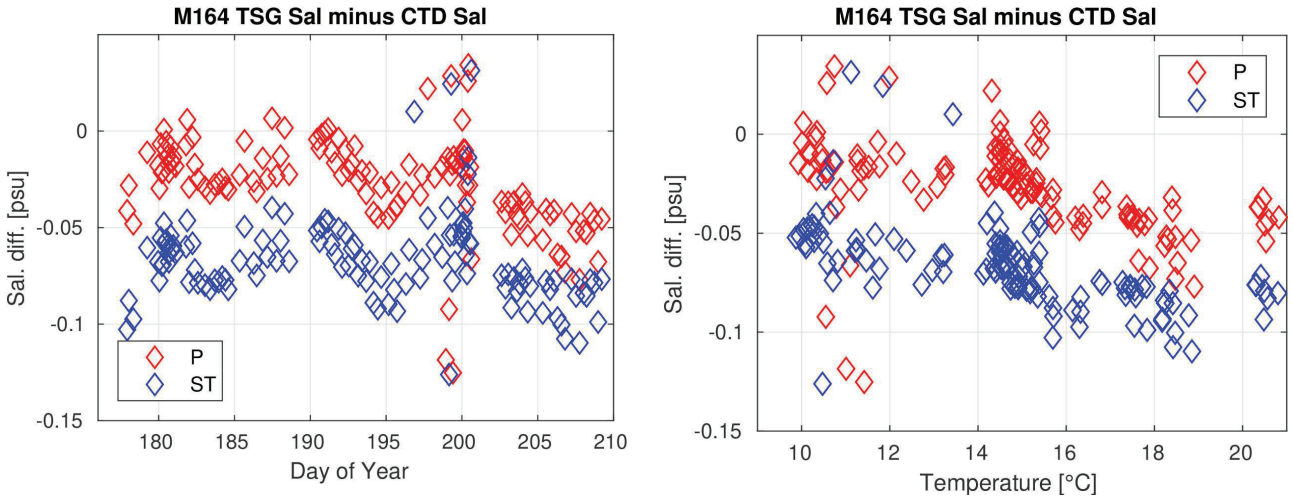

Fig. 5.22 Differences between TSG and CTD salinity as a function of time (left) and temperature (right) for both TSG systems (port- and starboard-side).

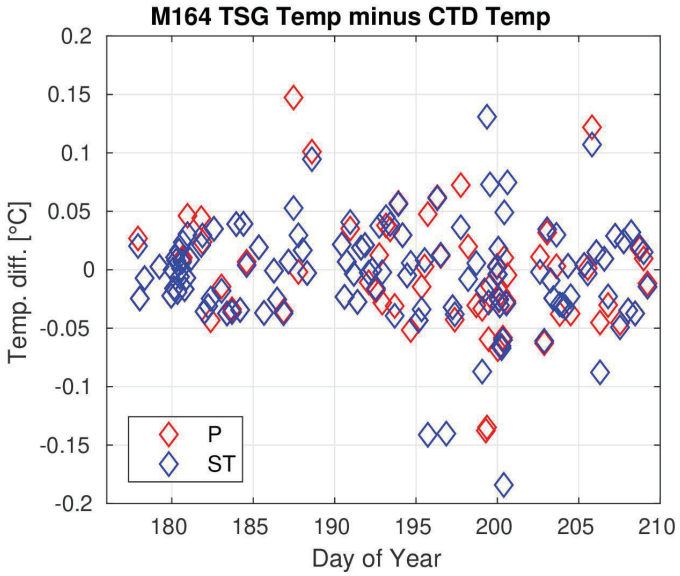

Fig. 5.23 Differences between TSG values and CTD temperature for both TSG systems (port- and starboard-side) over time.

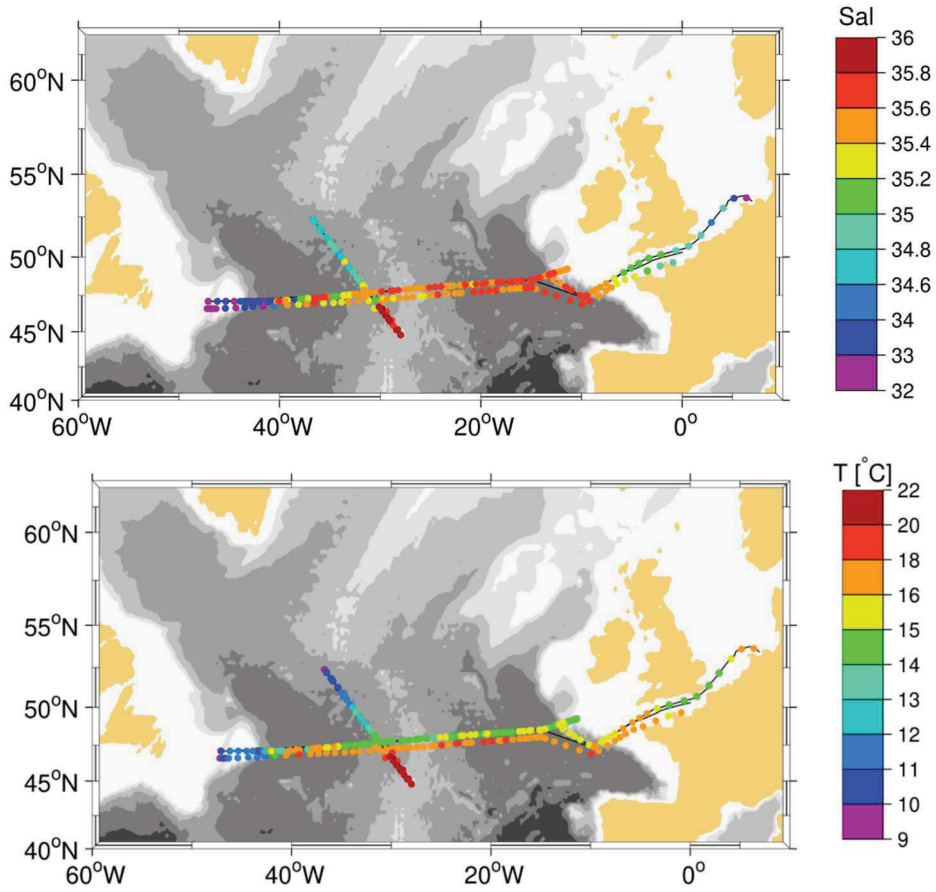

Fig. 5.24 Underway TSG measurements of salinity (top) and temperature (bottom). In order to allow a distinction of the data from the westward and eastward passage of the *R/V METEOR*, the data from the eastward (return) track are shifted southward by 0.5°.

Fig. 5.24 shows the underway TSG measurements of (calibrated) salinity and temperature. Relatively fresh surface waters are found in the North Sea, along the northern part of the Mid-Atlantic-Ridge section and west of 40°W, where the surface waters are influenced by the advection of fresh subarctic waters in the Labrador Current. There, and at the northern end of the Mid-Atlantic- Ridge section, also the coldest waters with temperatures of ~10°C have been encountered. Relatively warm surface waters are found in the western basin near the North Atlantic Current (~40°W), in the eastern basin and along the southern part of the Mid-Atlantic- Ridge section. On the way back from the west towards the North Sea, the temperatures are about 2°C higher than during the forward passage. This is probably the result of seasonal warming. The temperature increase is not accompanied by higher salinity; thus, an enhanced advection of subtropical waters seems unlikely.

5.8.2 In-Situ Aerosol Measurements

(O. Krüger*, M. Pöhlker*, B. Holanda*, M. Stelzner) * not onboard

A Wide Range Aerosol Spectrometer EDM 665 (WRAS) was operated during cruise *M164* in the subpolar Atlantic Ocean from July 03 until July 27, 2020. The WRAS consists of two instruments to measure aerosol size distributions from 5 nm to 32 µm with a time resolution < 3 minutes: (i) The Scanning Mobility Particle Sizer (SMPS+C) with a butanol condensation particle counter (CPC) for nanoparticles from 5 to 350 nm and (ii) the Environmental Dust Monitor (EDM 180) sizing the fraction from 0.25 to 32 µm. In addition, a standalone CPC was measuring the total aerosol number concentration (with 4 nm as lower cut off) in a 1 Hz time resolution. Among the aerosol measurements, basic associated meteorological data was captured such as humidity, pressure, wind speed, wind direction, and rain volume.

The data acquisition was done by using the SMPS+C, EDM 180 and CPC as well as the WRAS software from *GRIMM Aerosol Technik*. Pre-processed data from the GRIMM software as well as the raw data is available. The processed data is corrected for double charge as described by *Wiedensohler* (1988), the DMA transfer function and for diffusional wall loss of particles as described in e.g. *Rose et al.* (2008) and *Pöhlker et al.* (2016).

Figure 5.25 shows the total aerosol number concentration (top) and the aerosol size distribution with the particle diameter on the y-axis and the time on the x-axis, color-coded by the particle number concentration (bottom). Few hundred particles are measured, which fits to pan arctic marine background conditions *[Freud et al., 2017]*. The aerosol size distribution shows an Aitken mode of aerosol particles with diameters (D) between 5 nm and 50 nm (and accumulation mode particles with 50 nm < D > 500 nm. Most of the time both modes are present with similar number concentrations but also periods with only Aitken or only accumulation mode aerosol were measured. Remarkable is, the growth event from 10th of July until 13th of July. It seems that the *R/V METEOR* passed by the nucleation source because the growth appears in both directions (due to the sequence of a negative, followed by an absence and subsequent a positive growth rate). The total aerosol number shows some periods with very high concentrations. These episodes indicate

extra aerosol particles emitted from the vessel engines, blown in the direction of the WRAS or other anthropogenic emissions. These periods will be carefully checked and marked in the final dataset. The coarse mode particles, larger 500 nm stand for a small number fraction but a significant fraction of the aerosol mass and surface area. The total aerosol mass measured during this cruise ranges from values smaller than 0.5 µg per m³ up to values exceeding 100 µg per m³.

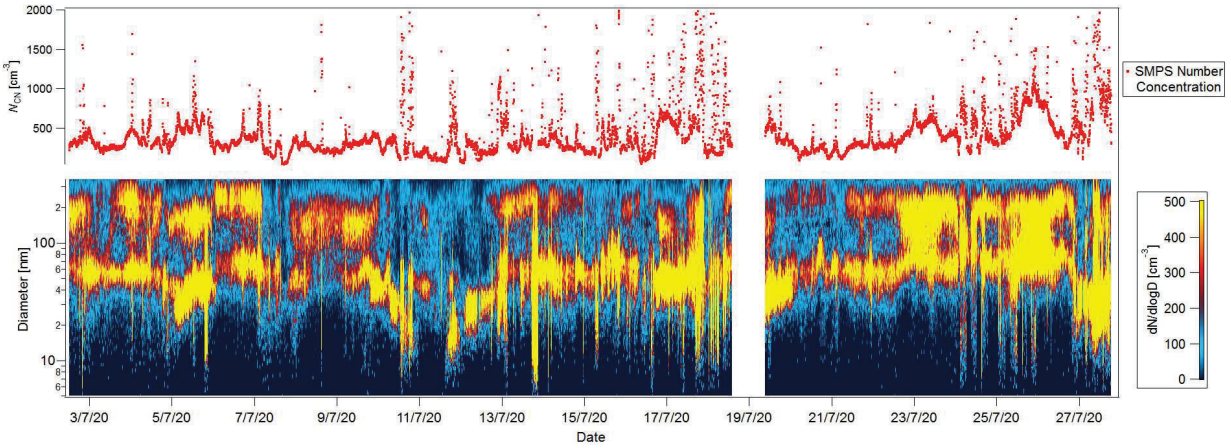

Fig. 5.25 Top: Integrated SMPS total number concentration (N_{cn}) data. Bottom: SMPS aerosol size distribution in the size range from 5 to 350 nm measured during cruise *M164*.

5.8.3 MICROTOPS Aerosol and Water Vapor Measurements

(S. Kinne*, A. Smirnov*, M. Stelzner) * not onboard

Reference for satellite remote sensing and global modeling are sparse over ocean regions. Thus, NASA's AERONET group distributes calibrated handheld (MICROTOPS) sun-photometers to sample aerosol properties and water vapor content. In contrast to often uncertain interpretations by satellite data, measurements of direct sun-light, when applied to an (by its location) exact solar background, yield highly accurate atmospheric properties. Solar measurements at five different solar spectral intervals allows (direct attenuation based) information on aerosol amount, on aerosol particles (e.g. pollution vs sea-salt or mineral dust) and on atmospheric water vapor content. Hereby, the water vapor content is determined by comparing the solar attenuation in a trace gas free spectral interval with the solar attenuation in a neighboring spectral interval affected by (known strength) water vapor absorption. The needed solar elevation information (to define the exact solar background) is provided by an attached GPS instrument. The samples are e-mailed at the end of each day into NASA's Marine Aerosol Network (MAN) database to serve from then on as reference data for satellite remote sensing retrievals and for global modeling.

MICROTOPS measurements require unobstructed views of the sun. Thus, measurements are only possible during the daytime, when views of the sun are not obstructed by clouds, by ship exhaust or ship obstructions. During an 8-second sub-sample, the instrument needs to be manually directed into the sun with the help of a pointing device. For a complete measurement, sub-samples

are requested to be immediately repeated 5 to 10 times (conditions permitting) to subsequently better identify and remove poor (higher attenuation) data due to cloud-contamination and/or instrument mis-orientation. Measurements are requested every 15 min, if possible.

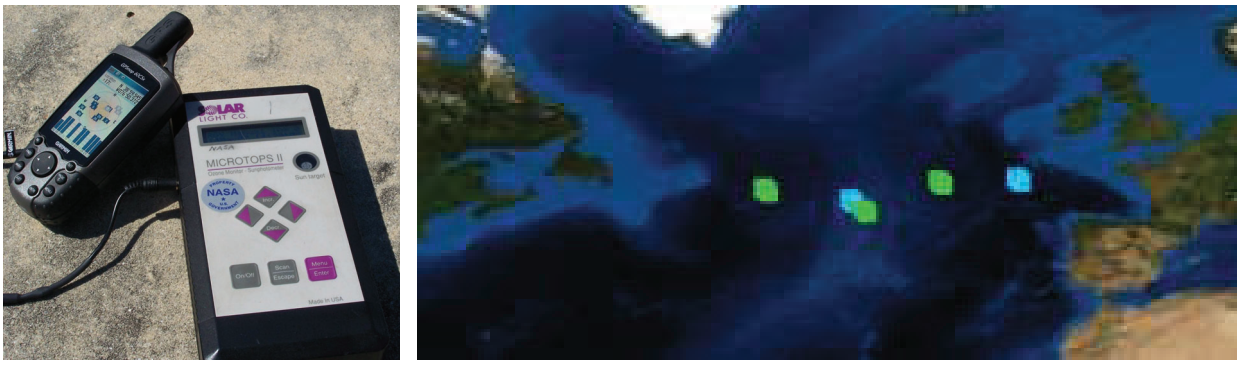

Fig. 5.26 The instrument (left) and daily averages of aerosol amount: the aerosol optical depth at 500nm. Blue dots indicate values below 0.1 and green dots between 0.1 and 0.2.

Results

All sampled data are immediately available to the entire science community via the web-page of the MAN database (http://aeronet.gsfc.nasa.gov/new_web/maritime_aerosol_network.html) – shortly after the data were transmitted via e-mail (at a day's end) to Alexander Smirnov (alexander.smirnov-1@nasa.gov). The aerosol and water vapor data collected during the *M164* cruise are available at https://aeronet.gsfc.nasa.gov/new_web/cruises_new/Meteor_20_1. Via the '*Download Data and Track*' button, not only data on aerosol amount (aerosol optical depth: AOD) and water vapor but also derived properties are offered (as the AOD fine-mode fraction, via the AOD spectral dependence). Recorded daily AOD averages are presented in Figure 5.26.

6 Ship's Meteorological Station

(M. Stelzner)

After 2 months in the shipyard, the research vessel (R/V) *METEOR* left the port of Emden on June 23 around 7 o'clock UTC. On the upcoming cruise, a CTD section was planned from the marine region southwest of Ireland westwards to the Canadian EEZ off Newfoundland. Halfway along the route, this section was to be interrupted to allow another CTD-section of approximately 550 nm length to the northwest.

At the beginning of the voyage, a large-scale high-pressure system with centre over the German Bight provided calm weather conditions. The wind blew with a maximum of 4 Bft from southeast to east directions. The sea state was not worth mentioning until crossing the Strait of Dover around

noon on June 24, when a low swell from the west arrived. In total, the transit through the North Sea and the English Channel lasted three days, and the research area was reached at noon on June 26.

In the meantime, a slowly deepening low-pressure complex extended from Western Europe across the British Isles to the sea area south of Iceland, with the actual centre near 50°N, 14°W. The centre of this low-pressure system shifted to the Hebrides and then remained almost stationary for several days, whereby the core pressure further deepened somewhat. This led to unstable and windy conditions in the sailing area: The westerly wind increased to 6 Bft, and the sea state rose to 2.5 m.

In the following days, a new low-pressure complex extended from southeast Greenland across the British Isles to Scandinavia. Smaller embedded low-pressure systems and associated fronts repeatedly swept across *R/V METEOR*'s operation area. Rain showers and occasionally prolonged periods of rain were the order of the day. The wind changed repeatedly from prefrontal 5-6 Bft from southwest to postfrontal 4 Bft from northwest. With thick cloud cover and a fog field in the afternoon of June 29 the sun was hardly visible.

From July 01 onwards, another low centre shifted from the sea area west of *R/V METEOR* to the Irminger Sea. At the same time, a strong Azores high expanded. During this time, the operating area was situated within a strong southwesterly current. The mean wind reached its maximum on July 04 with 7 to 8 Bft. Due to the strong wind, the wind sea also increased, so that the combined significant wave height reached 3.5-4 m on July 04. The swell came from southwest to west.

On July 05, the one-and-a-half-day transit to the most northwestern point of the described northwestern-CTD-section began. Over the following 5 days, this section was worked off to the southeast. During this period, *R/V METEOR* twice passed through a distinct low-pressure zone extending from 51°37'N, 31°41'W in a southwesterly direction up to Bermuda. Several low centres and the ex-tropical storm named *Edouard* were embedded in this trough. This very complex weather situation created variable conditions. Depending on the position of the ship within this low-pressure zone, the wind sometimes blew from the southwest with 5-6 Bft, in between it calmed down, sometimes it rose to 5-6 Bft from the northeast. A similar pattern was observed in sea state, varying between 1 m in the frontal zone and 2.5 m at the edge of the depression, combined with several variable swells from northern and southern directions. In addition to the chaotic wind and sea state conditions, rain and foggy phases were also present.

From July 11 to July 18, the second part of the CTD-west-section was completed. During this period, *R/V METEOR* was almost continuously on the western edge of a stable Azores high in a very constant, humid and unstable southwest current. While approaching Newfoundland, these conditions caused a fog phase lasting several days. During this period, the wind mostly blew with 4 Bft, occasionally also with 5 Bft. The sea state was 1.5 m, the swell run in from southeastern to southern directions. During the cruise there were neither any icebergs in the research region, nor was the cruise affected by any sea ice tongue on or near the Canadian shelf break.

On July 18, the west-section was finally completed, and the transit towards the east began. In the period from July 20 to July 27, it was interrupted repeatedly by individual CTD stations. During the whole period, *R/V METEOR* was located between a high south of the cruise area and several northeast moving low-pressure systems north of the cruise area and thus in a steady southwest to west current. Only the passage of associated fronts with embedded rain showers caused short northwesterly wind periods. The wind speed remained at 4 to 5 Bft, the sea state at 1.5 m. On July 26, a small low moved over *R/V METEOR* for the last time. The wind rose to 7 and, for a short time, also to 8 Bft, which increased the sea state to 2.5 m.

When reaching the English Channel on the evening of July 28, the research was officially terminated. At this time, a high-pressure system spread from France to Great Britain and moved eastwards together with the *R/V METEOR*. Associated weak winds from southwest and a hardly detectable sea state were very similar to the beginning of the voyage. At noon of July 31, *R/V METEOR* reached the mouth of the river Ems, and four hours later cruise *M164* ended in the port of Emden.

Additional information

During the cruise there were neither any icebergs in the research region, nor was the cruise affected by any sea ice tongue on or near the Canadian shelf break.

Due to technical problems the wind sped values were incorrectly calculated between 06/23/2002, 07:13 UTC and 06/26/2020, 20:15 UTC. The DWD data set has been corrected. Unfortunately, the data set directly stored and contained in the DSHIP system of the vessel cannot be corrected and shows incorrect values for this period.

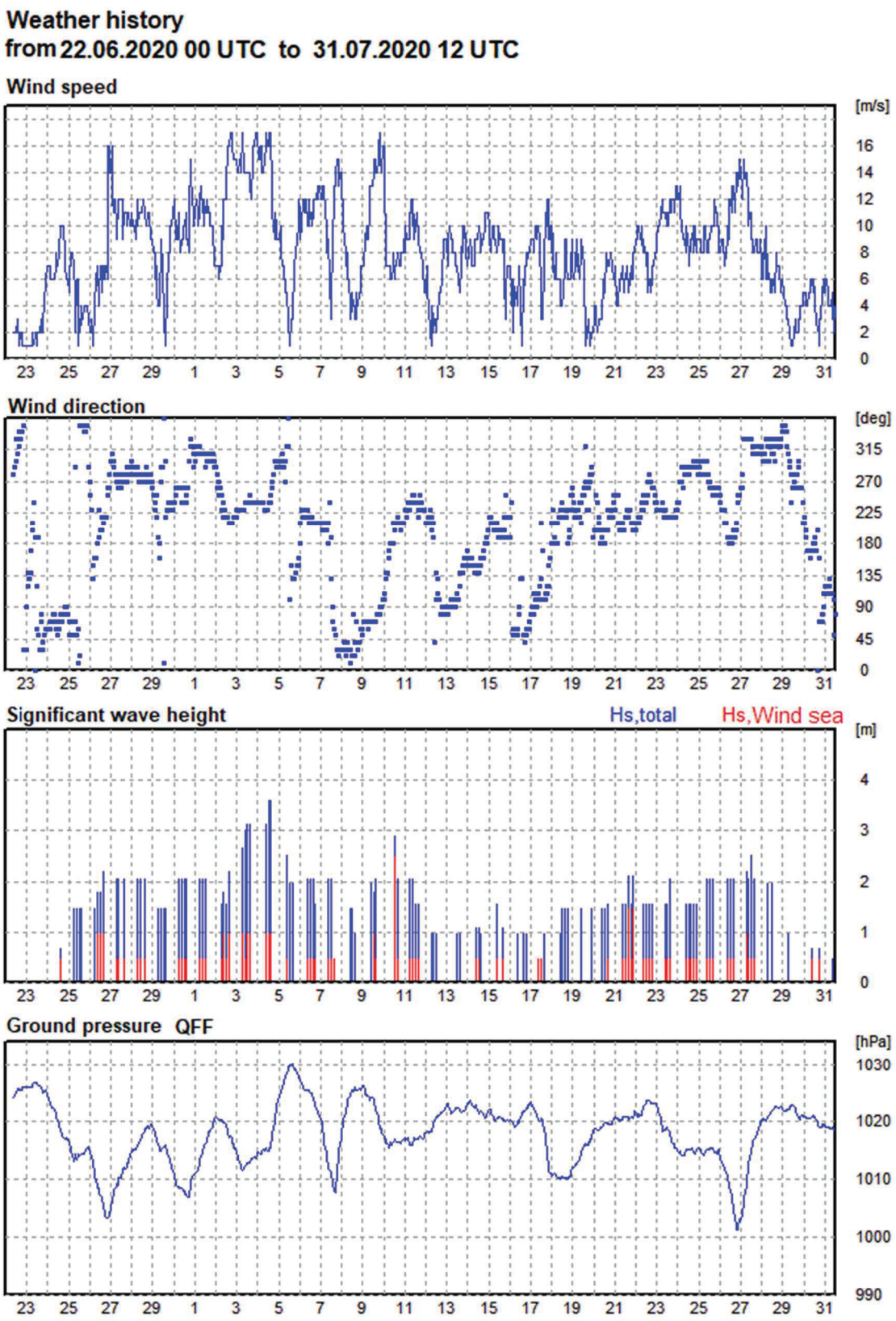

Fig. 6.1 Meteorological conditions observed during June 23 and July 31, 2020, cruise *M164*.

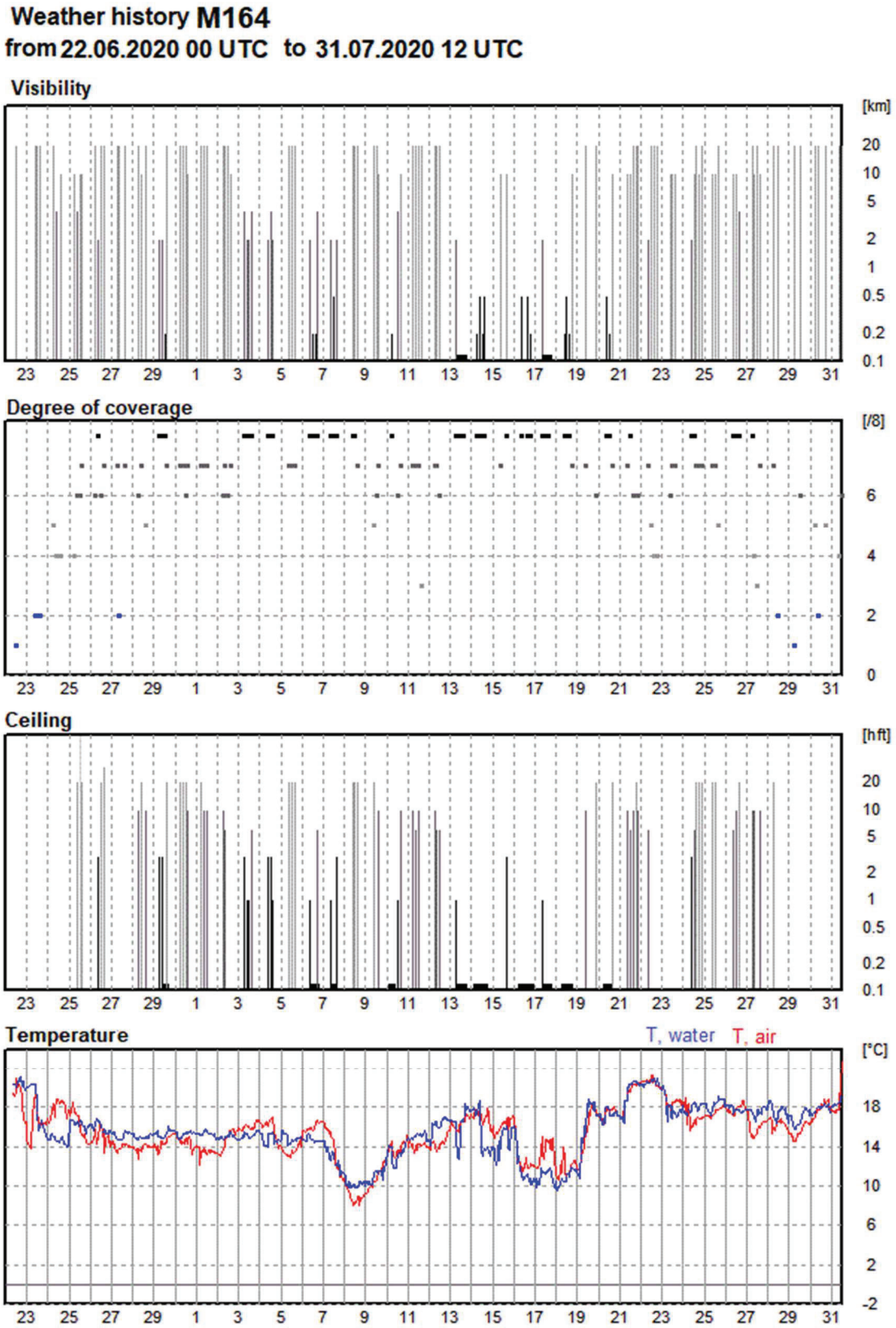

Fig. 6.2 Meteorological conditions observed during June 23 and July 31, 2020, cruise *M164*, continued.

Figure 6.1 and 6.2 provide an overview on the atmospheric conditions recorded throughout the cruise by the sensors of weather station installed on the vessel's mast. Figure 6.3 displays the spatial distribution of absolute wind speeds and directions (hourly values) along the cruise track. Periods of absolute wind speeds exceeding 7 Bft were only rarely observed.

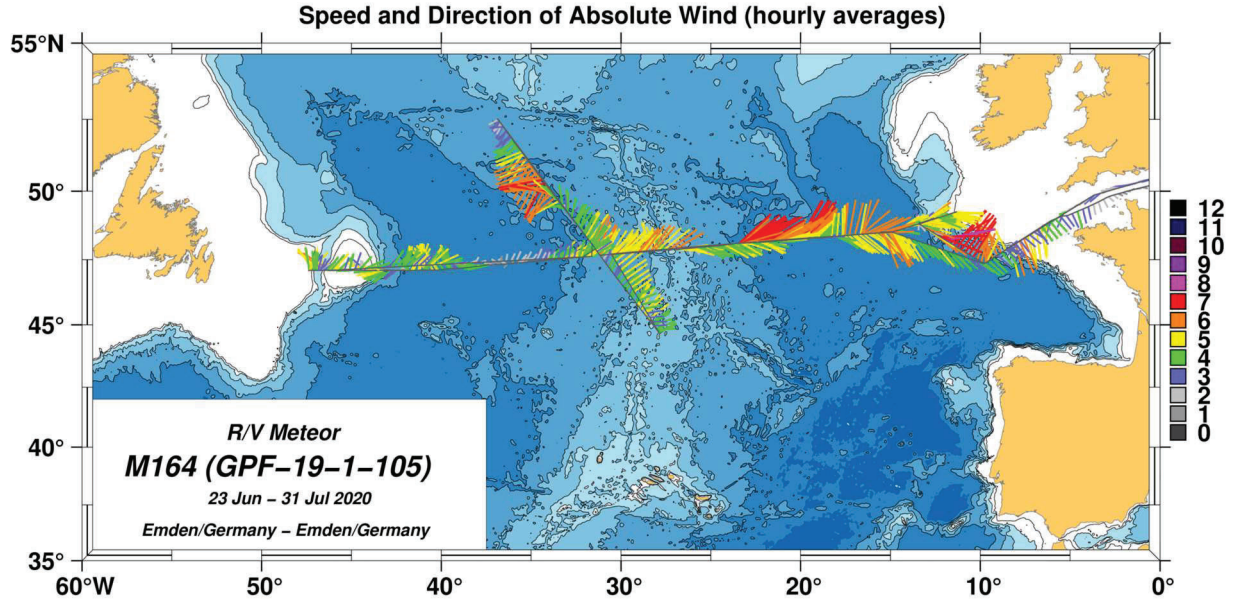

Fig. 6.3 Spatial distribution of hourly wind speeds and directions observed during cruise *M164*. Values are reported on the Beaufort scale. Figure by D. Kieke.

7 Station List *M164*

Station	Profile	Date	Time [UTC]	Latitude	Longitude	Water Depth [m]	Profile Depth [m]	SF6/CFC	Bottle Oxygen	LADCP	Remarks
M164_1-1	1	2020/06/25	21:34	47°53.68'N	08°30.89'W	2700	2664	x	x	x	
M164_1-2	2	2020/06/26	00:22	47°53.67'N	08°30.91'W	2692	1979	-	-	x	Test of acoustic releases
M164_2-1	3	2020/06/26	07:24	47°23.03'N	09°39.96'W	4380	3461	-	x	x	MicroCAT calibration
M164_3-1	4	2020/06/27	04:52	48°49.80'N	13°25.39'W	4454	4436	x	x	x	
M164_4-2	5	2020/06/27	22:33	48°59.44'N	12°37.62'W	1600	1587	x	x	x	
M164_5-1	6	2020/06/28	00:36	49°01.56'N	12°26.51'W	1283	1267	x	x	x	
M164_6-1	7	2020/06/28	02:37	49°04.74'N	12°11.67'W	1014	994	x	x	x	
M164_7-1	8	2020/06/28	04:27	49°07.77'N	11°56.56'W	855	845	x	x	x	
M164_8-1	9	2020/06/28	06:15	49°11.01'N	11°41.71'W	790	779	x	x	x	
M164_9-1	10	2020/06/28	08:09	49°14.14'N	11°26.67'W	465	452	-	x	x	
M164_10-1	11	2020/06/28	09:46	49°15.71'N	11°19.33'W	281	268	-	-	x	
M164_11-1	12	2020/06/28	11:26	49°12.59'N	11°34.21'W	620	618	-	x	x	
M164_12-1	13	2020/06/28	13:16	49°09.42'N	11°49.08'W	797	785	x	x	x	
M164_13-1	14	2020/06/28	15:05	49°06.25'N	12°03.98'W	920	906	-	-	x	
M164_13-2	15	2020/06/28	16:04	49°06.25'N	12°03.98'W	920	794	x	x	x	Argos beacon test
M164_14-1	16	2020/06/28	17:56	49°03.12'N	12°18.97'W	1135	1121	x	x	x	
M164_15-1	17	2020/06/28	20:37	48°58.49'N	12°41.12'W	1775	1761	x	x	x	
M164_16-1	18	2020/06/28	23:03	48°56.86'N	12°48.77'W	2096	2074	x	x	x	MicroCAT and RBR calibration
M164_17-1	19	2020/06/29	02:23	48°53.77'N	13°03.78'W	3627	260	-	-	x	Profile aborted
M164_20-1	20	2020/06/29	18:40	48°55.60'N	12°56.99'W	2624	2594	x	x	x	
M164_21-1	21	2020/06/29	21:03	48°53.84'N	13°03.74'W	3629	3612	x	x	x	
M164_22-1	22	2020/06/30	00:07	48°51.71'N	13°13.79'W	3757	3732	x	x	x	
M164_23-1	23	2020/06/30	04:47	48°44.91'N	13°48.38'W	4532	4515	x	x	x	
M164_24-1	24	2020/06/30	09:07	48°40.18'N	14°10.90'W	4550	4530	x	x	x	
M164_25-1	25	2020/06/30	13:31	48°35.49'N	14°33.20'W	4698	4682	x	x	x	
M164_26-2	26	2020/07/01	01:07	48°31.05'N	15°00.02'W	4813	4796	x	x	x	
M164_27-1	27	2020/07/01	08:39	48°28.56'N	16°01.87'W	4836	4822	x	x	x	

Station	Profile	Date	Time [UTC]	Latitude	Longitude	Water Depth [m]	Profile Depth [m]	SF6/CFC	Bottle Oxygen	LADCP	Remarks
M164_28-1	28	2020/07/01	15:52	48°25.32'N	17°02.27'W	4204	4152	x	x	x	
M164_29-1	29	2020/07/01	22:29	48°22.03'N	18°02.69'W	4512	4492	x	x	x	
M164_30-1	30	2020/07/02	03:50	48°20.53'N	18°46.92'W	4355	4339	x	x	x	
M164_31-1	31	2020/07/02	09:18	48°18.68'N	19°31.23'W	4565	4552	x	x	x	
M164_32-1	32	2020/07/02	14:07	48°17.11'N	19°59.97'W	4436	4415	x	x	x	
M164_33-1	33	2020/07/03	07:37	48°15.80'N	20°29.85'W	4180	4163	x	x	x	
M164_34-1	34	2020/07/03	15:26	48°12.73'N	21°28.49'W	4456	4438	x	x	x	
M164_35-2	35	2020/07/04	05:46	48°06.95'N	23°24.54'W	4509	4487	x	x	x	
M164_36-1	36	2020/07/04	11:05	48°08.44'N	22°47.82'W	4200	4185	x	x	x	
M164_37-1	37	2020/07/04	20:22	48°05.11'N	23°54.91'W	4094	4078	x	x	x	
M164_38-1	38	2020/07/05	04:00	48°01.68'N	25°07.44'W	3887	3868	x	x	x	
M164_39-1	39	2020/07/05	11:13	47°57.53'N	26°20.00'W	3078	3039	x	x	x	
M164_40-1	40	2020/07/05	17:47	47°53.34'N	27°32.51'W	3423	3358	x	x	x	
M164_41-1	41	2020/07/06	00:28	47°49.16'N	28°45.16'W	2750	2700	x	x	x	
M164_42-1	42	2020/07/06	06:43	47°45.03'N	29°57.82'W	3495	3469	x	x	x	
M164_43-1	43	2020/07/06	13:45	47°40.08'N	31°08.34'W	4100	4075	x	x	x	
M164_44-1	44	2020/07/08	10:18	52°30.55'N	36°51.97'W	3375	3341	x	x	x	
M164_45-1	45	2020/07/08	13:48	52°18.87'N	36°37.38'W	3714	3688	x	x	x	
M164_46-1	46	2020/07/08	17:26	52°06.86'N	36°23.13'W	3341	3316	x	x	x	
M164_47-1	47	2020/07/08	23:00	51°42.43'N	35°54.56'W	3432	3415	x	x	x	
M164_48-1	48	2020/07/09	04:09	51°18.20'N	35°25.55'W	3698	3685	x	x	x	
M164_49-1	49	2020/07/09	09:20	50°53.67'N	34°56.73'W	3516	3512	x	x	x	
M164_50-1	50	2020/07/09	14:28	50°29.44'N	34°28.03'W	4060	4034	x	x	x	
M164_51-1	51	2020/07/09	19:55	50°05.13'N	33°59.29'W	4240	4227	x	x	x	
M164_52-1	52	2020/07/10	01:38	49°40.72'N	33°30.37'W	3997	3989	x	x	x	
M164_53-1	53	2020/07/10	06:47	49°16.40'N	33°01.49'W	3801	3792	x	x	x	
M164_54-1	54	2020/07/10	11:54	48°52.01'N	32°32.68'W	3840	3824	x	x	x	
M164_55-1	55	2020/07/10	16:52	48°27.67'N	32°03.63'W	4211	4191	x	x	x	
M164_56-1	56	2020/07/10	22:06	48°03.35'N	31°35.06'W	3943	3924	x	x	x	
M164_57-1	57	2020/07/11	02:52	47°37.48'N	31°37.46'W	3760	3745	x	x	x	

Station	Profile	Date	Time [UTC]	Latitude	Longitude	Water Depth [m]	Profile Depth [m]	SF6/CFC	Bottle Oxygen	LADCP	Remarks
M164_58-1	58	2020/07/11	09:26	47°34.46'N	32°34.68'W	3953	3953	x	x	x	
M164_59-1	59	2020/07/11	15:46	47°30.87'N	33°32.12'W	4138	4087	x	-	x	
M164_60-1	60	2020/07/11	22:00	47°27.27'N	34°29.50'W	4299	4396	x	x	x	
M164_61-1	61	2020/07/12	04:03	47°23.56'N	35°27.07'W	4180	4309	x	x	x	
M164_62-1	62	2020/07/12	09:56	47°20.07'N	36°24.32'W	4224	4228	x	x	x	
M164_63-1	63	2020/07/12	15:37	47°17.78'N	37°22.37'W	4489	4507	x	x	x	
M164_64-1	64	2020/07/13	02:56	47°15.08'N	37°56.65'W	4570	4589	x	x	x	
M164_65-1	65	2020/07/13	07:37	47°12.40'N	38°31.06'W	4619	4610	x	x	x	
M164_66-1	66	2020/07/13	12:20	47°10.24'N	39°01.08'W	4588	4584	x	x	x	
M164_67-1	67	2020/07/13	16:41	47°09.80'N	39°28.40'W	4586	4579	x	x	x	MicroCAT and NKE calibration
M164_68-1	68	2020/07/14	06:41	47°06.59'N	40°11.26'W	4561	4554	x	x	x	
M164_69-1	69	2020/07/14	12:13	47°06.57'N	40°52.64'W	4502	4478	x	x	x	
M164_70-1	70	2020/07/14	19:49	47°05.95'N	41°15.44'W	4442	4417	x	x	x	
M164_71-1	71	2020/07/15	04:57	47°05.61'N	41°37.69'W	4296	4279	x	x	x	
M164_72-1	72	2020/07/15	09:03	47°05.24'N	41°59.54'W	4229	4212	x	x	x	
M164_73-1	73	2020/07/15	17:30	47°06.25'N	42°16.31'W	4009	3995	x	x	x	
M164_75-1	74	2020/07/16	03:56	47°06.09'N	42°35.49'W	3676	3654	x	x	x	
M164_77-1	75	2020/07/16	16:27	47°06.05'N	42°53.65'W	3473	3443	x	x	x	
M164_78-1	76	2020/07/16	19:29	47°06.08'N	43°07.07'W	3516	3549	x	x	x	
M164_79-1	77	2020/07/16	22:15	47°06.17'N	43°13.35'W	3049	3030	x	x	x	
M164_80-1	78	2020/07/17	00:46	47°06.02'N	43°17.85'W	2680	2562	-	x	x	
M164_81-1	79	2020/07/17	02:48	47°05.90'N	43°20.17'W	1846	1788	x	x	x	
M164_82-1	80	2020/07/17	04:31	47°06.00'N	43°25.25'W	1291	1268	x	x	x	
M164_83-1	81	2020/07/17	06:29	47°05.99'N	43°38.35'W	777	755	x	x	x	
M164_84-1	82	2020/07/17	07:48	47°05.99'N	43°47.42'W	597	572	x	x	x	
M164_85-1	83	2020/07/17	09:24	47°06.07'N	44°02.53'W	363	345	-	-	x	
M164_86-1	84	2020/07/17	11:00	47°05.59'N	44°17.94'W	250	235	-	-	x	
M164_87-1	85	2020/07/17	12:33	47°06.04'N	44°31.25'W	162	151	-	-	x	
M164_88-1	86	2020/07/17	22:40	47°05.66'N	47°22.80'W	245	228	-	-	x	
M164_89-1	87	2020/07/17	23:27	47°05.75'N	47°19.45'W	313	293	x	x	x	

Station	Profile	Date	Time [UTC]	Latitude	Longitude	Water Depth [m]	Profile Depth [m]	SF6/CFC	Bottle Oxygen	LADCP	Remarks
M164_90-1	88	2020/07/18	00:17	47°05.90'N	47°15.83'W	483	463	-	-	x	
M164_91-1	89	2020/07/18	01:11	47°05.98'N	47°12.49'W	737	716	x	x	x	
M164_92-1	90	2020/07/18	02:14	47°05.92'N	47°09.27'W	893	863	-	-	x	
M164_93-1	91	2020/07/18	03:15	47°05.90'N	47°05.84'W	1035	1012	x	x	x	
M164_94-1	92	2020/07/18	04:30	47°06.05'N	47°00.56'W	1137	1113	-	-	x	
M164_95-1	93	2020/07/18	06:05	47°06.04'N	46°51.16'W	1181	1155	x	x	x	
M164_96-1	94	2020/07/18	07:33	47°05.97'N	46°42.48'W	1148	1124	-	-	x	
M164_97-1	95	2020/07/18	08:41	47°06.08'N	46°40.01'W	1106	1083	x	x	x	
M164_98-1	96	2020/07/18	10:03	47°06.08'N	46°36.67'W	821	799	-	-	x	
M164_99-1	97	2020/07/18	11:18	47°06.09'N	46°33.25'W	503	484	x	x	x	
M164_100-1	98	2020/07/18	12:37	47°06.12'N	46°24.17'W	363	343	-	-	x	
M164_101-1	99	2020/07/18	14:24	47°06.04'N	46°08.45'W	336	317	-	-	x	
M164_102-1	100	2020/07/20	14:24	47°36.24'N	32°06.03'W	4050	4074	-	x	x	MicroCAT & Aquadopp calibration
M164_103-1	101	2020/07/20	20:30	47°53.82'N	31°25.68'W	3882	3867	-	x	x	
M164_104-1	102	2020/07/21	01:08	47°32.55'N	31°02.27'W	3710	3695	-	x	x	
M164_105-1	103	2020/07/21	05:42	47°11.27'N	30°38.53'W	3607	3589	x	x	x	
M164_106-1	104	2020/07/21	10:11	46°49.90'N	30°14.85'W	3087	3087	x	x	x	
M164_107-1	105	2020/07/21	14:31	46°28.58'N	29°51.16'W	3125	3122	x	-	x	
M164_108-1	106	2020/07/21	18:57	46°07.29'N	29°27.54'W	3125	3144	x	x	x	
M164_109-1	107	2020/07/21	23:21	45°45.95'N	29°03.87'W	3275	3274	x	x	x	
M164_110-1	108	2020/07/22	03:38	45°24.68'N	28°40.19'W	2648	2640	x	x	x	
M164_111-1	109	2020/07/22	07:35	45°03.36'N	28°16.53'W	2219	2226	-	x	x	
M164_112-1	110	2020/07/22	11:30	44°42.00'N	27°52.89'W	1405	1432	x	-	x	
M164_113-1	111	2020/07/23	06:58	47°41.66'N	30°31.21'W	3518	3501	-	x	x	
M164_114-1	112	2020/07/23	13:05	47°45.40'N	29°21.13'W	3061	3040	-	x	x	
M164_115-1	113	2020/07/23	19:15	47°49.34'N	28°08.50'W	2392	2407	-	x	x	
M164_116-1	114	2020/07/24	00:56	47°53.40'N	26°53.12'W	2834	2763	-	x	x	
M164_117-1	115	2020/07/24	06:39	47°57.27'N	25°40.47'W	3352	3378	-	x	x	
M164_118-1	116	2020/07/24	12:48	48°01.02'N	24°30.45'W	4040	4030	-	x	x	
M164_119-1	117	2020/07/24	19:06	48°06.74'N	23°24.42'W	4493	4486	-	x	x	

Station	Profile	Date	Time [UTC]	Latitude	Longitude	Water Depth [m]	Profile Depth [m]	SF6/CFC	Bottle Oxygen	LADCP	Remarks
M164_120-1	118	2020/07/25	05:18	48°08.57'N	22°10.29'W	4455	4447	-	x	x	
M164_121-1	119	2020/07/25	12:22	48°12.37'N	21°00.13'W	4238	4193	-	x	x	
M164_122-1	120	2020/07/25	17:37	48°14.77'N	20°16.01'W	4416	4412	-	x	x	
M164_123-1	121	2020/07/26	00:24	48°18.64'N	19°03.29'W	4011	4008	-	x	x	
M164_124-1	122	2020/07/26	05:09	48°20.45'N	18°29.58'W	4591	4589	-	x	x	
M164_125-1	123	2020/07/26	11:01	48°23.56'N	17°32.45'W	4232	4227	-	x	x	
M164_126-1	124	2020/07/26	16:48	48°26.60'N	16°35.26'W	4805	4803	-	x	x	
M164_127-1	125	2020/07/26	23:19	48°29.98'N	15°32.96'W	4838	4830	-	x	x	
M164_128-1	126	2020/07/27	05:09	48°31.84'N	14°56.67'W	4813	4810	-	x	x	

8 Data and Sample Storage and Availability

After the end of cruise *M164*, all meta information, underway, and bathymetric data was sent to the German Oceanographic Data Centre (DOD) at BSH, which inventoried the respective cruise summary report and the data under reference number 20200099 (https://www.bsh.de/EN/DATA/Climate-and-Sea/Oceanographic_Data_Center/Cruise_summary_reports/_Module/HTML/2020_node.html). The bathymetric data centre at BSH stores the raw data obtained from the *EM122*-multibeam system under the data set number M164.202006 (https://www2.bsh.de/daten/DOD/Bathymetrie/Nordatlantik/m164.htm). Multibeam data was also sent to the *Deutsche Allianz Meeresforschung* (DAM), and respective raw data is provided via the PANGAEA database, https://doi.org/10.1594/PANGAEA.927172.

Already aboard, raw and processed scientific oceanic data was merged into the data collections of the University of Bremen and the BSH Hamburg, which facilitates any exchange of data products and results among project partners. All scientific data is immediately available to project partners and can be obtained on request by interested cooperating scientists.

Scientific data of cruise *M164* will be made public and submitted to international data centres like the CLIVAR & Carbon Hydrographic Data Office (cchdo.ucsd.edu) and PANGAEA (www.pangaea.de) at the end of quarter 2 of year 2023. Both serve as open access long-term archives providing free access to the scientific data. Contact persons are Dr. Reiner Steinfeldt (hydrography/tracers, rsteinf@physik.uni-bremen.de), Prof. Monika Rhein (Bremen moorings/PIES, mrhein@uni-bremen.de), Dr. Christian Mertens (ADCP, cmertens@uni-bremen.de), Dr. Kerstin Jochumsen (BSH moorings, kerstin.jochumsen@bsh.de).

Coarse-resolution (5 dbar) calibrated CTDO data of the upper 4000 dbar range were sent already during the cruise to the *Coriolis* data centre at *Ifremer*, Brest, France. There, they will be used in the quality-control of Argo data and integrated into operational ocean models (data recipient: codata@ifremer.fr). All Argo data were collected and immediately made freely available by the International Argo Program and the national programs that contribute to it (http://www.argo.ucsd.edu, http://argo.jcommops.org). The Argo program is part of the *Global Ocean Observing System* (GOOS). Contact person for the BSH core Argo floats deployed during the cruise is Dr. Birgit Klein (birgit.klein@bsh.de), contact person for the deployed *Ifremer* Deep Argo floats is Dr. Damien Desbruyères (damien.desbruyeres@ifremer.fr). Float data of the cruise can be accessed via https://fleetmonitoring.euro-argo.eu/dashboard?Cruise=M164.

Contact person for the WRAS data is Dr. Mira Pöhlker (m.pohlker@mpic.de), contact person for the MICROTOPS measurements is Dr. Stefan Kinne (stefan.kinne@mpimet.mpg.de).

9 Acknowledgements

We would like to express our gratitude to the master of *R/V METEOR*, Rainer Hammacher, and his entire crew for the assistance and great support granted to us during cruise *M164 (GPF-19-1-105)*. We have greatly appreciated the very friendly working environment, the hospitality experienced onboard the vessel, and the very professional and constructive cooperation between the different scientific teams and the ship's team. We further thank Barbara Kozak, Wolfgang Böke, and Jürgen Stake at our home laboratory and Peter Brackmann and Alina Bozdharaj (Uni Bremen, FB-2) for assistance in the preparation of the cruise, the Federal Ministry for Education and Research (BMBF) through the cooperative research program *RACE-Synthesis* and the *Geschäftsstelle des Gutachterpanels Forschungsschiffe* (GPF) of the *German Research*

Foundation (DFG). The latter two provided the funding and necessary ship time to pursue all scientific work. We particularly acknowledge the support of the *German Research Fleet Coordination Centre* (Leitstelle Deutsche Forschungsschiffe) and *Briese Research* in the preparation of this cruise. We furthermore acknowledge Ulrich Drübbisch and Andreas Welsch, both at IfM Hamburg, for providing backup instruments, Tim Fischer at GEOMAR, Kiel, for providing the OSSI toolbox for MATLAB, and Andreas Thurnherr at LDEO, USA, for making the LADCP processing software LDEO-IX_13 available to the public.

10 References

Bulsiewicz, K., H. Rose, O. Klatt, A. Putzka, and W. Roether (1998), A capillary-column chromatographic system for efficient chlorofluorocarbon measurement in ocean waters. *J. Geophys. Res.*, 103, 15959-15970, doi:10.1029/98JC00140.

Dutton, G., J. Elkins II, B. Hall, and NOAA ESRL (2017), Earth System Research Laboratory Halocarbons and Other Atmospheric Trace Gases Chromatograph for Atmospheric Trace Species (CATS) Measurements, Version 1. [insitu_global_F12.txt, insitu_global_SF6.txt]. NOAA National Centers for Environmental Information. doi:10.7289/V5X0659V [accessed on 17 Jan 2020].

Freud E. et al. (2017), Pan-Arctic aerosol number size distributions: seasonality and transport patterns, *Atmos. Chem. Phys.,* 17, 8101–28, doi:10.5194/acp-17-8101-2017.

GEBCO Compilation Group (2020), GEBCO 2020 Grid, doi:10.5285/a29c5465-b138-234d-e053-6c86abc040b9.

Pöhlker, M. L. et al. (2016), Long-term observations of cloud condensation nuclei in the Amazon rain forest – Part 1: Aerosol size distribution, hygroscopicity, and new model parametrizations for CCN prediction, *Atmos. Chem. Phys.*, 16, 15709–15740, doi:10.5194/acp-16-15709-2016.

Rose, D. et al. (2008), Calibration and measurement uncertainties of a continuous-flow cloud condensation nuclei counter (DMT-CCNC): CCN activation of ammonium sulfate and sodium chloride aerosol particles in theory and experiment, *Atmos. Chem. Phys.*, 8, 1153–1179, doi:10.5194/acp-8-1153-2008.

Thurnherr, A. (2018), How to process LADCP data with the LDEO software, Versions IX.7 – IX.13, January 17, 2018, available at http://www.ldeo.columbia.edu/cgi-bin/ladcp-cgi-bin/hgwebdir.cgi/LDEO_IX.

Visbeck, M. (2002), Deep velocity profiling using lowered acoustic Doppler current profilers: Bottom track and inverse solutions, *J. Atmos. Oceanic Technol.*, 19, 794–807, doi:10.1175/1520-0426(2002)019<0794:DVPULA>2.0.CO;2.

Wiedensohler, A. (1988), An approximation of the bipolar charge distribution for particles in the submicron size range, *J. Aerosol Sci.*, 19, 387–389, doi:10.1016/0021-8502(88)90278-9.